Astron Astrophys Rev (2024)32:3
https://doi.org/10.1007/s00159-024-00154-z

REVIEW ARTICLE

Experimental studies of black holes: status and future prospects

Reinhard Genzel[1,2,3] · Frank Eisenhauer[1,4] · Stefan Gillessen[1]

Received: 27 February 2024 / Accepted: 21 March 2024

Abstract

More than a century ago, Albert Einstein presented his general theory of gravitation (GR) to the Prussian Academy of Sciences. One of the predictions of the theory is that not only particles and objects with mass, but also the quanta of light, photons, are tied to the curvature of space-time, and thus to gravity. There must be a critical compactness, above which photons cannot escape. These are black holes (henceforth BH). It took 50 years after the theory was announced before possible candidate objects were identified by observational astronomy. And another 50 years have passed, until we finally have in hand detailed and credible experimental evidence that BHs of 10 to 10^{10} times the mass of the Sun exist in the Universe. Three very different experimental techniques, but all based on Michelson interferometry or Fourier-inversion spatial interferometry have enabled the critical experimental breakthroughs. It has now become possible to investigate the space-time structure in the vicinity of the event horizons of BHs. We briefly summarize these interferometric techniques, and discuss the spectacular recent improvements achieved with all three techniques. Finally, we sketch where the path of exploration and inquiry may go on in the next decades.

Keywords Black holes · Galactic center · Interferometry · GRAVITY

Contents

Extended author information available on the last page of the article

Published online: 25 April 2024

1 *Presto:* Theoretical background

A '*black hole*' (e.g., Wheeler 1968) conceptually is a region of space-time where gravity is so strong that within its *event horizon* neither particles with mass, nor even electromagnetic radiation, can escape from it. Based on Newton's theory of gravity and assuming a corpuscular nature of light, Michell (1784) and Laplace (1795) were the first to note that a sufficiently compact, massive star may have a surface escape velocity exceeding the speed of light. Such an object would thus be 'dark' or invisible. A proper mathematical treatment of this remarkable proposition had to await Albert Einstein's theory of General Relativity in 1915/1916 (Einstein 1916, henceforth GR). Karl Schwarzschild's (1916) first analytic solution of the vacuum field equations in spherical symmetry revealed the unavoidable existence of a characteristic *event horizon* in the *metric* of a mass M, the *Schwarzschild radius* $R_{\rm s} = 2\,GM/c^2 = 2\,R_{\rm g}$ (with the gravitational radius $R_{\rm g} = GM/c^2$), within which no communication is possible with external observers. It is a 'one way door'. Radially inward moving observers, after crossing the event horizon, cannot stop, nor reverse back out, but end up in finite 'Eigenzeit' (proper time) at the center. All the mass/energy of a BH is concentrated there in a central singularity.

Kerr (1963) generalized this solution to spinning BHs. For the normalized spin parameter $(0 \leq \chi \leq 1)$ the event horizon becomes

$$R_{\rm event\ horizon} = \frac{GM}{c^2} \times \left(1 + (1-\chi^2)^{1/2}\right). \tag{1}$$

Newman (1965) found the axisymmetric solution for a BH that is both rotating and electrically charged. Israel, Carter, Robinson, Wheeler, Bekenstein and Ruffini then formulated the so-called '*no-hair theorem*' (1967–1975),[1] stating that *a stationary BH solution is completely described by the three parameters of the Kerr–Newman metric: mass, angular momentum, and electric charge*. For the Kerr metric this means that the quadrupole moment Q_2 of the BH is determined by the spin, namely $Q_2/M = -\chi^2$. However, these solutions refer to configurations with sufficiently high symmetry, so that Einstein's equations can be solved analytically. This led to a debate whether the conclusions obtained were generally applicable. Penrose (1963, 1965) dropped the assumption of spherical symmetry, and analyzed the problem topologically. Using the key concept of '*trapped surfaces*' he showed that any arbitrarily

[1] See Israel (1967), Carter (1971), Robinson (1975) and Bekenstein (1975).

shaped surface with a curvature radius less than the Schwarzschild radius is a trapped surface. Any observer is then inexorably pulled towards the center where time ends.

The distortion of the space-time outside the event horizon leads to a minimum radius, where stable circular orbits are possible. For particles with mass this *innermost stable, circular orbital radius* (ISCO) is $6\,R_{\rm g} = 3\,R_{\rm S}$ for $\chi = 0$, and $R_{\rm g}$ for $\chi = 1$. For photons of no mass this innermost stable orbital radius (called *photon orbit*) is $3\,R_{\rm g} = 1.5\,R_{\rm S}$ for $\chi = 0$, and $R_{\rm g}$ for $\chi = 1$ (Bardeen et al. 1972). Finally, if a BH is irradiated by a point source at large distance behind the BH, only photons with projected radii $\geq 3\sqrt{3}R_{\rm g}$ arrive at the distant observer in front of the BH. Those inside form a '*shadow*' (a central depression of light, Bardeen et al. 1972; Luminet 1979; Falcke et al. 2000) and do not reach the observer.

Work by Bardeen, Bekenstein, Carter, and Hawking in the early 1970s[2] led to the formulation of *BH thermodynamics*. These laws describe the behavior of a BH in close analogy to the laws of classical thermodynamics, by relating mass to energy, area to entropy, and surface gravity to temperature. The analogy was completed when Hawking (1974) showed that quantum field theory implies that BHs should emit particles and photons like a black body with a temperature proportional to the surface gravity of the BH, hence inversely proportionally to its mass. This predicted effect is now known as *Hawking radiation*'. For the astrophysical BHs discussed here, the Hawking radiation is out of reach of current detection methods by many orders of magnitude.

From considerations of the *information content* of BHs, there is significant tension between the predictions of GR and general concepts of quantum theory (e.g., Susskind 1995; Maldacena 1998; Bousso 2002). It is likely that a proper quantum theory of gravity will modify the concepts of GR on scales comparable to or smaller than the *Planck length*, $l_{\rm Pl} = \sqrt{\frac{\hbar G}{c^3}} \sim 1.6 \times 10^{-33}$ cm, remove the concept of the central singularity, and potentially challenge the interpretation of the GR event horizon (Almheiri et al. 2013). If gravity is fundamentally a higher-dimensional interaction, then the fundamental Planck length in 3D can be substantially larger (Arkani-Hamed et al. 1998).

But are these bizarre objects of GR (and science fiction) actually realized in Nature? The ultimate question discussed in the following is not just whether the weak-field gravity region near compact objects is qualitatively consistent with the BH geometry of GR, but rather to quantify the limits of observations (= experiments at a distance) in testing the existence of event horizons (cf. Cardoso and Pani 2019, and references therein). "How close" is a self-gravitating object to a BH? One can introduce a *"closeness" parameter* ϵ, *such that* $\epsilon \rightarrow 0$ *corresponds to the BH limit*. For example one can choose the compactness, such that for a spherically symmetric space time

$$\epsilon = 1 - \frac{2\,GM/c^2}{R} \tag{2}$$

where M is the object mass in the static case and R is its radius (cf. Cardoso and Pani 2019). Likewise, one can introduce ϵ as a measure of the violation of the no-hair theorem above. Alternatives of the GR BH proposal for compact astrophysical

[2] See Christodoulou (1970), Christodoulou and Ruffini (1971), Carter (1971), Bardeen et al. (1973), Bardeen (1973), Hawking (1974) and Bekenstein (1975).

objects are '*exotic compact objects*' ('ECOs', Cardoso and Pani 2019; Psaltis 2024). These might be concentrations of heavy, dark matter bosons or fermions, such as '*boson stars*' (Torres et al. 2000), or '*fermion balls*' (Viollier et al. 1993; Tsiklauri and Viollier 1998; Becerra-Vergara et al. 2020), or '*gravastars*' (stars supported by negative vacuum pressure, e.g., Mazur and Mottola 2004; Cardoso and Pani 2019), or '*wormholes'* (Morris and Thorne 1988; Cardoso and Pani 2019).

2 *Vivace:* X-ray binaries and quasars

Astronomical evidence for the existence of BHs started to emerge 60 years ago with the discovery of variable X-ray emitting binary stars in the Milky Way (Giacconi et al. 1962; Giacconi 2003) on the one hand, and of distant, luminous 'quasi-stellar-radio-sources/objects' (*quasars* or *QSO*s, Schmidt 1963) on the other. Dynamical mass determinations from Doppler spectroscopy of the visible primary star established that the mass of the X-ray emitting secondary is sometimes significantly larger than the maximum stable neutron star mass, ~ 2.3 solar masses (McClintock and Remillard 2006; Remillard and McClintock 2006; Özel et al. 2010; Rezzolla et al. 2018). The binary X-ray sources thus are excellent candidates for stellar BHs (SBH, ~ 8–$20\,M_{\odot}$). If so they are probably formed when a massive star explodes as a supernova at the end of its fusion lifetime and the compact remnant collapses to an SBH.

The radio to X-ray luminosities of quasars often exceed by 3 to 4 orders of magnitude the entire energy output of the Milky Way Galaxy. Furthermore, their strong high-energy emission in the UV-, X-ray and γ-ray bands, as well as their spectacular relativistic jets, can most plausibly be explained by accretion of matter onto rotating (super)-massive BHs (henceforth (S)MBHs, 10^6–$10^{10}\,M_{\odot}$, e.g., Lynden-Bell 1969; Shakura and Sunyaev 1973; Blandford and Znajek 1977; Rees 1984; Blandford 1999; Yuan and Narayan 2014; Blandford et al. 2019). Between 5.7% (for a non-rotating Schwarzschild hole) and 42% (for a maximally rotating Kerr hole) of the rest energy of infalling matter can, in principle, be converted to radiation outside the event horizon. This efficiency is two orders of magnitude greater than nuclear fusion in stars. To explain powerful QSOs by this mechanism, BH masses of 10^8 to 10^{10} solar masses, and accretion flows between 0.1 to tens of solar masses per year are required. Often the accretion rate is expressed as *Eddington ratio*, where a value of 1 corresponds to the situation that the radiation pressure of the emission equals the gravitational pull of the MBH.

Quasars are located (without exception) in the nuclei of large, massive galaxies (e.g., Osmer 2004). Quasars represent the most extreme and spectacular among the general nuclear activity of most galaxies (Netzer 2015). There may also be intermediate mass BHs (IMBHs, 10^2–$10^5\,M_{\odot}$), for instance in the cores of globular clusters or dwarf galaxies. Evidence for $> 10^5\,M_{\odot}$ MBHs in low mass galaxies is growing but the case for IMBHs in globular clusters is still very much debated (Greene et al. 2020). Finally, there have been proposals that BHs with a wide mass spectrum might have been created in the rapid cool-down phase after the Big Bang (e.g., Carr and Hawking 1974; Carr 1975; Hasinger 2020).

A conclusive experimental proof of the existence of a BH, as defined by GR, requires the *determination of the gravitational potential at or near the scale of the event horizon*. This gravitational potential can be inferred from spatially resolved measurements of the motions of test particles (interstellar gas, stars, other BHs, or photons) in close trajectory around the BH (Lynden-Bell and Rees 1971), or from gravitational waves emitted in the inspiral of a binary BH. Lynden-Bell (1969) and Lynden-Bell and Rees (1971) proposed that (S)MBHs might be common in most galaxies (although in a low state of accretion). If so, dynamical tests are feasible in nearby galaxy nuclei, including the center of our Milky Way. Because of the small angular radius of the event horizon (e.g., 10 micro-arcsec for the 4.3 million solar mass MBH even in the 'nearby', 8.27 kpc, Galactic Center), achieving the necessary instrumental resolution requires *extremely large telescopes (or spatial interferometers) with exquisite sensitivity and spectral resolution*.

Over the past 50 years, increasingly solid *evidence for central 'dark' (i.e., non-stellar) mass concentrations* has emerged for more than several hundred galaxies in the local Universe (e.g., Magorrian et al. 1998; Gebhardt et al. 2000; Ferrarese and Merritt 2000; Kormendy 2004; Gültekin et al. 2009; Fabian 2012; Kormendy and Ho 2013; McConnell and Ma 2013; Saglia et al. 2016; Greene et al. 2013, 2016). The data come from optical/infrared imaging and spectroscopy on the Hubble Space Telescope (HST, and most recently from the James Webb Telescope (JWST)), from large ground-based telescopes, as well as from Very Long Baseline radio Interferometry (VLBI). Further evidence comes from relativistically broadened, redshifted iron Kα line emission in nearby Seyfert galaxies (e.g., Tanaka et al. 1995; Nandra et al. 1997; Fabian and Iwasawa 2000), including the first statistical constraints on the BH spin distribution (Reynolds 2021).

In external galaxies a compelling case that such a dark mass concentration cannot just be a dense nuclear cluster of white dwarfs, neutron stars and perhaps stellar BHs, already emerged in the mid-1990s from spectacular VLBI observations of the nucleus of NGC 4258. This is a mildly active galaxy at a distance of 7 Mpc (Miyoshi et al. 1995; Moran 2008). The VLBI observations show that the galaxy nucleus contains a thin, slightly warped disk of H_2O masers (viewed almost edge on), in beautiful Keplerian rotation around an unresolved mass of 40 million solar masses, as inferred from the maser motions. The maser motions exceed 1000 km/s at the innermost edge of the disk of about 0.1 pc. The inferred density of this mass exceeds a few 10^9 solar masses pc^{-3} and thus cannot be a long-lived cluster of 'dark' astrophysical objects of the type mentioned above (Maoz 1995). Greene et al. (2013) presented a survey of such H_2O disk maser MBHs. As we will discuss below, the Galactic Center provides a yet more compelling case.

In the galaxies investigated, dark masses are found ranging from a few 10^4 to $10^5\,M_\odot$ in low mass systems (Greene et al. 2020), to $10^{10+}\,M_\odot$ in very massive spheroidal/elliptical galaxies (Kormendy and Ho 2013; McConnell and Ma 2013). For the ellipticals and for galaxies with 'classical' bulges (Kormendy and Kennicutt Jr 2004), there appears to be a fairly low scatter relationship between central mass and bulge mass (Häring and Rix 2004; Kormendy and Ho 2013; McConnell and Ma 2013). About 0.2–0.7% of the bulge mass is in the central dark mass, increasing

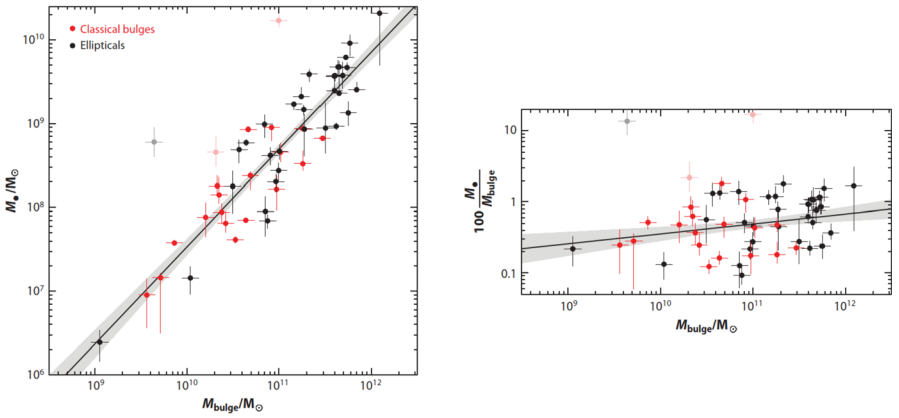

Fig. 1 Relationship between inferred central mass (from stellar and gas dynamics) $M_\bullet$ and bulge mass in local Universe massive galaxies (ellipticals, or disks with classical bulges). There clearly is a correlation between these two components, with a best fit $\frac{M_\bullet}{M_{bulge}} = (4.9 \pm 0.6) \times 10^{-3} \times \left(\frac{M_{bulge}}{10^{11} M_\odot}\right)^{0.14 \pm 0.08}$ (adapted from Fig. 18 of Kormendy and Ho 2013)

slowly with bulge mass, and strongly suggesting that central dark mass and bulge have grown together over cosmological time scales (Fig. 1).

3 *Allegro:* Testing the MBH paradigm in the Galactic Center with stellar orbits and radio emission

The central light years of our Galaxy contain a dense and luminous star cluster, as well as several components of neutral, ionized and extremely hot gas (Fig. 2; Genzel and Townes 1987; Genzel et al. 1994; Morris and Serabyn 1996; Melia and Falcke 2001; Genzel et al. 2010; Morris et al. 2012). Compared to the distant quasars, the Galactic Center is 'just around the corner' ($R_0 = 8.27$ kilo-parsecs (kpc), 27 000 light years). High resolution observations of the Milky Way nucleus thus offer the unique opportunity of carrying out a stringent test of the MBH-paradigm deep within its gravitational 'sphere of influence' where gravity is dominated by the central mass ($R < 1 - 3$ pc). Since the center of the Milky Way is highly obscured by interstellar dust particles in the plane of the Galactic disk, observations in the visible part of the electromagnetic spectrum are not possible. The veil of dust, however, becomes transparent at longer wavelengths (the infrared, microwave and radio bands), as well as at shorter wavelengths (hard X-ray and γ-ray bands), where observations of the Galactic Center thus become feasible (Oort 1977).

3.1 Initial statistical evidence for a compact central mass from gas and stellar motions

Starting in the late 1970s/1980s, observations of the Doppler motions of ionized and neutral gas clouds in the central parsecs (Wollman et al. 1977; Lacy et al. 1980;

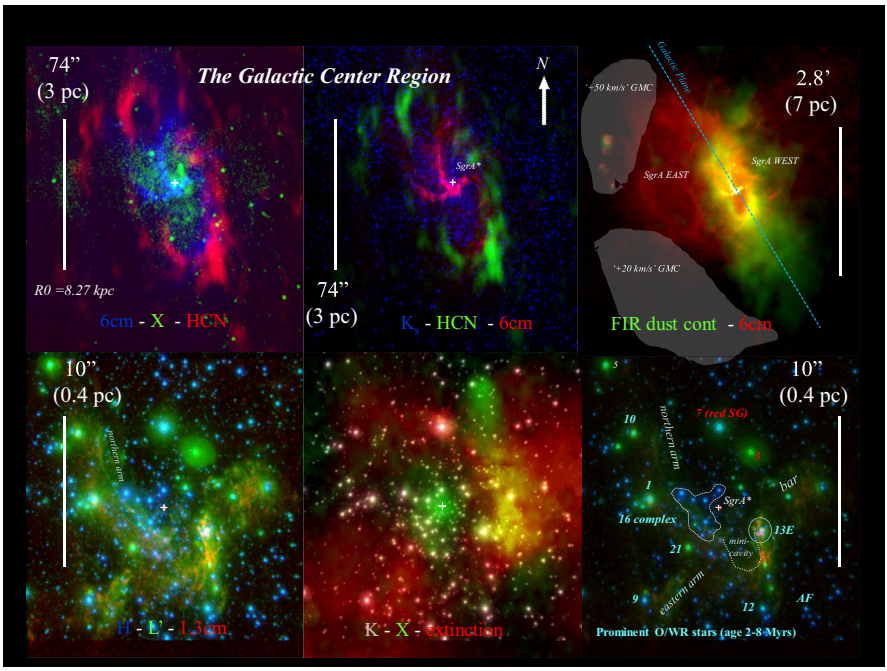

Fig. 2 Summary of the different components: stars (old giants, red and blue super-giants), cold (20–200 K) molecular/neutral gas and dust, ionized (10^4 K) and hot (1–10 × 10^6 K) gas, and their distributions on sub-parsec, to 10 parsec scale in the Galactic Center (adapted from Genzel et al. 2010). The cross in the center of the images marks the location of the compact, non-thermal radio source SgrA*, probably a MBH of 4.3 million solar masses (Genzel et al. 2010). Top right: Largest scales of the SgrA region, with the HII region SgrA WEST and the supernova remnant SgrA EAST (presumably an explosion of one or several massive O/Wolf–Rayet star(s) ∼20–40 000 years ago. Outside of this region are two giant molecular clouds at '+20' and '+50' km/s LSR velocity. Top left and center: zoom in onto SgrA WEST, which harbors the center of a dense ($\rho_* > 10^6\, M_\odot\, \mathrm{pc}^{-3}$) cluster of old, and young, massive stars. The central 1.5-pc diameter region is filled with ionized gas streamers (bottom left), hot X-ray emitting gas (bottom center), and the most massive, recently formed O, Wolf–Rayet and B-stars (bottom right). Winds and UV-radiation from these stars and the MBH have created a lower density 'cavity' relatively devoid of dense molecular gas and dust (average hydrogen density $n_H \sim 10^{3..4.5}\ \mathrm{cm}^{-3}$). The central cavity in turn is surrounded by a rotating, clumpy 'circum-nuclear' ring of warm dust and dense, molecular gas (HCN and other high excitation gas components are found here, and the molecular hydrogen density is $n_{H2} \sim 10^{5-6}\ \mathrm{cm}^{-3}$, Becklin et al. 1982; Ho 1995). Gas is streaming in and out of the central region in form of clumpy, tidally disrupted 'streamers', such as the 'northern' and 'eastern' arms and the 'bar' (cf. Oort 1977; Lo and Claussen 1983; Genzel and Townes 1987; Ho et al. 1991; Genzel et al. 1994; Melia and Falcke 2001; Genzel et al. 2010; Morris et al. 2012)

Serabyn and Lacy 1985; Crawford et al. 1985), and of stellar velocities (McGinn et al. 1989; Krabbe et al. 1995; Haller et al. 1996) found the first evidence for a central mass concentration of a few million solar masses, concentrated on or near the compact radio source SgrA*. In the 1990s observations of stellar proper motions with the telescopes of the European Southern Observatory (ESO) in Chile (Eckart and Genzel 1996; Genzel et al. 1997), and with the Keck telescopes on Mauna Kea (Ghez et al. 1998) further improved the statistical and systematic evidence. Yet in terms of the compactness parameter ϵ introduced in the first paragraph, these early

measurements did not provide significant evidence that this mass concentration must be a BH: $0 \ll \epsilon \sim 1\text{–}10^{-5}$. It could instead be a cluster of faint stars, neutron stars, or stellar BHs.

3.2 Sharper images and individual stellar orbits on solar system scales

Further progress required three new key elements. One is much higher angular resolution and integral-field imaging spectroscopy (achieved with 8–10 m telescopes, and aided by adaptive optics to reach the diffraction limit of $\sim$50–60 milli-arcsec). These improvements were realized both in Chile (ESO-VLT) and in Hawaii (Keck) between 2000 and 2005. The second are very long duration observation campaigns (>1–2 decades) to observe not only stellar velocities, but derive the full orbital parameters of individual stars as precision tracers of the potential. The third was luck, namely to find stars much closer to SgrA* than was theoretically expected (i.e., on solar system scales. cf. Alexander 2005, 2017).

The most important scientific breakthrough started in 2002 when both the ESO-VLT (Schödel et al. 2002) and the Keck telescope (Ghez et al. 2003) discovered that the star S2 (or S02 in UCLA nomenclature) approached SgrA* to about 15 milli-

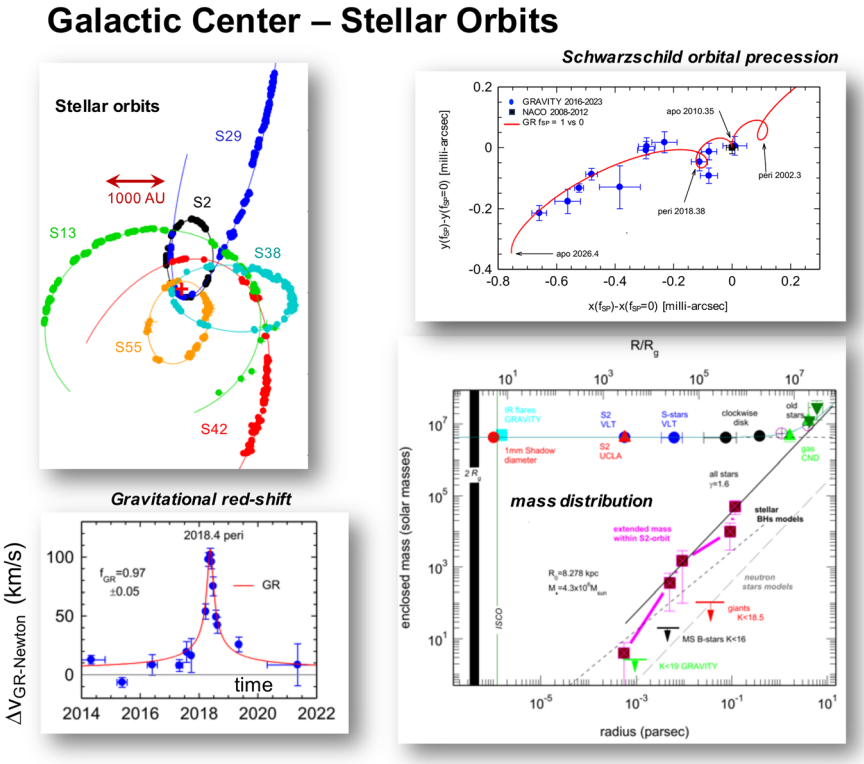

Fig. 3 Tests of the MBH paradigm and GR in the Galactic Center using individual stellar orbits

arcsec (~ 15 light hours or 1200 R_S), and sharply turned around SgrA* on a highly elliptical orbit ($e = 0.88$). By 2010, both the VLT- and the Keck-based groups were able to derive orbits for about 10–20 stars remarkably close to SgrA* (top left panel of Fig. 3, Ghez et al. 2008; Gillessen et al. 2009), followed in the next decade by steady progress in the number and stars and quality of their derived orbital parameters (Boehle et al. 2016; Gillessen et al. 2017). Now the observations were able to exclude the compact star cluster hypothesis, but a few speculative alternative explanations to a MBH, such as 'boson' or 'fermion' stars (see Sects. 1, 6) still were possible. And in any case, there also remained the theoretical possibility that GR was not applicable, since not yet tested in the MBH regime.

3.3 Interferometry and detection of post-Newtonian orbital deviations

The next big breakthrough started in 2016/2017 with the completion and continuous further improvements of the GRAVITY (GRAVITY Collaboration et al. 2017) and GRAVITY+ (GRAVITY+ Collaboration et al. 2022) infrared interferometric beam combiner of the 4×8 m telescopes of the ESO-VLT (https://www.mpe.mpg.de/ir/gravity, Fig. 12 left panel, GRAVITY Collaboration et al. 2022b; Eisenhauer et al. 2023). GRAVITY(+) achieves a near-infrared resolution of about 3 milli-arcsec, and an astrometric precision of 10–100 micro-arcseconds, about 10–20 times better than with individual 10 m-class telescopes, and has polarization, spectroscopic, and wide and deep imaging modes (GRAVITY Collaboration et al. 2017, 2022a, 2024; GRAVITY+ Collaboration et al. 2022, 2024).

With the combined new instrumental capabilities, precision measurements of ~ 50 stellar orbits (central panel) of the so-called S-stars around SgrA* determine the central mass and its distance to the Sun to be 4.300 (± 0.011 (1σ statistical), ± 0.018 (1σ systematic)) $\times 10^6\, M_\odot$, and $R_0 = 8273$ (± 7.5, ± 15) pc, centered on the position of SgrA* (Boehle et al. 2016; Gillessen et al. 2017; Do et al. 2019a; GRAVITY Collaboration et al. 2019a, 2022b, 2024). The stellar orbits set stringent limits to any additional mass in the vicinity, of a few thousand solar masses within a few $10^4\, R_S$ (bottom-right panel), as determined by the orbital data of ~ 15 stars (Gillessen et al. 2017; Do et al. 2019a; GRAVITY Collaboration et al. 2019a, 2022b, a, 2023b; Evans et al. 2023; Will et al. 2023).

This conclusion is also supported the near-pericenter astrometric orbit of S2, after subtracting the best fitting Newtonian orbit. While Newton's theory would thus expect these positions to lie in an inclined highly elliptical orbit centered on SgrA*, GR in contrast predicts that the stellar motions exhibit a prograde in-plane precession, the '*Schwarzschild*'-precession, with an advance of

$$\Delta\Phi(\text{per orbit}) = 3\pi f_{\text{SP}} \frac{R_S}{a(1-e^2)}.$$

For the 16-year orbit of S2 ($a = 0.125''$, or 1039 AU, $e = 0.884$, $R_{\text{peri}}/R_S = a(1-e)/R_S = 1200$) this precession is 12.1' per orbit in clockwise direction. In the framework of post-Newtonian (PPN) expansions (Johannsen 2016), the Schwarzschild precession is first order in $(v/c)^2$, or a few times 10^{-4}. GR has

$f_{\rm SP} = 1$, while Newton has $f_{\rm GR} = 0$. The top right panel of Fig. 3 shows the location of the averaged S2 residual data obtained with GRAVITY (filled blue circles) and NACO (VLT adaptive optics imaging, black cross), after removing the Newtonian best-fit orbit. In this presentation the precession predicted by GR turns into the loopy red line. The observed data points are in excellent agreement with the GR prediction (the data in Fig. 3 give $f_{\rm SP} = 1.2 \pm 0.1$). This represents a confirmation that GR is correct in the space-time environment of a 4 million solar mass concentration; it also confirms that this mass concentration is compact and not a centrally peaked, but spatially extended distribution (GRAVITY Collaboration et al. 2020b, 2022b). Most of the mass is in a single concentrated object. Any nearby second (intermediate mass) BH companion ($< 10^3$ AU, or $10\,R_{\rm peri}$ of the stars S2 and S29), can only have a mass of $< 10^3\,M_\odot$ (GRAVITY Collaboration et al. 2023b; Will et al. 2023). In PPN=1.5 ($\sim (v/c)^3$) GR has a second orbital precession, the *Lense–Thirring* precession per orbit is

$$\Delta\Phi_{\rm LT} = 2\chi \times \left(\frac{R_{\rm S}}{a(1-e^2)}\right)^{1.5},$$

around the spin axis of the MBH. For the star S2, the Lense–Thirring precession is about $0.0497 \times \chi$ (arcminutes/orbit), for a spin parameter $\chi(\leq 1)$, so at least 240 times smaller than the star's Schwarzschild precession, and out of reach of the current astrometry.

GR also has a PPN=1 order effect in line of sight velocity, the *gravitational redshift*, of 100 km/s for S2. The bottom left inset of Fig. 3 shows the residual Doppler velocity of the star S2 as a function of time around the peri-approach in 2018.4, relative to that predicted by a Newtonian orbit of the same orbital parameters (horizontal gray line). The red curve are the residuals curve predicted by GR. The actual observed residuals are the blue filled circles. Our yield $f_{\rm GR} = 0.97 \pm 0.05$ (in addition to another 100 km/s redshift due to the transverse Doppler effect), again in excellent agreement with GR ($f_{\rm GR} = 1.0$, GRAVITY Collaboration et al. 2018a, 2020b; Do et al. 2019a).

Further tests of General Relativity near a MBH GRAVITY Collaboration et al. (2019b) confirmed the Equivalence Principle in the orbit of S2 through a test of the linear positional invariance. In that paper the redshift data are split into spectroscopy of the hydrogen Brγ line and the HeI 2.1μm line, and the gravitational redshift term is computed for the two data sets. Einstein's Equivalence Principle stipulates that in free fall the motion should only depend on mass/energy, and not on composition. And indeed, GRAVITY Collaboration et al. (2019b) set an upper limit of a few 10^{-2} to the fractional difference of the gravitational redshift in hydrogen and helium. In another paper, Hees et al. (2017, 2020) used the Galactic Center data to set limits on a hypothetical fifth force, and variations in the fine structure constant. (Jovanović et al. 2024) analyzed the Schwarzschild precession of S2 in the framework of Yukawa gravity theory, and set an upper limit to the mass of the graviton, which is compatible with limits from aLIGO gravitational-wave data.

Near event horizon motions and strong magnetic fields The near-IR emission from SgrA* itself is linearly polarized ($\sim 40\%$, Eckart et al. 2006a, b; Genzel et al. 2010)

and is synchrotron emission from very hot gas in the accretion zone, like the radio emission. The near-IR emission is constantly varying, with a red-noise power spectrum (Do et al. 2009; Dodds-Eden et al. 2009, 2010, 2011; Witzel et al. 2012, 2018). The power spectrum is typically log-normal, but occasionally high amplitude 'flares' above occur over a few hours at >10–20 times the average quiescent level (Dodds-Eden et al. 2009, 2011; Do et al. 2019b; Genzel et al. 2010). These flares exhibit 'clockwise' orbital motion on a scale of 8–9 R_g, just outside the EHT ring (GRAVITY Collaboration et al. 2018b, 2023a). The polarization direction also exhibits rotation at the same rate and in the same direction as the astrometric motions. GRAVITY Collaboration et al. (2023a) conclude that the accretion zone must be within a few tens of degrees of face-on. The polarization properties clearly show that the near-event horizon accretion zone is magnetically dominated with a dominant poloidal field (Fig. 4: left panel, GRAVITY Collaboration et al. 2018b, 2020c, a, 2023a; Wielgus et al. 2022). The accretion flow in the Galactic Center thus is a variant of the 'MAD' flows ($B \sim$ 80–100 G, Yuan and Narayan 2014; Bower et al. 2018; Dexter et al. 2020; Ressler et al. 2020b).

The hot gas density in the accretion zone around SgrA* is comparably low, $n_e \sim$ a few 10^3 cm^{-3} at a few $10^3\,R_g$ (Gillessen et al. 2019), and $n_e \sim$ a few 10^6 cm^{-3} at $\geq 10\,R_g$ (Marrone et al. 2007; Quataert 2004). The accretion flow in the Galactic Center thus is *radiative inefficient* and hot, since the density is too low to equilibrate the electron and ionic accretion fluids (Rees 1984; Quataert and Gruzinov 2000; Yuan et al. 2003; Yuan and Narayan 2014). These properties are consistent with strongly sub-Eddington accretion ($10^{-8\ldots-9}\,M_\odot$ year^{-1}, Baganoff et al. 2003; Blandford and Begelman 1999; Gillessen et al. 2019 and references therein). If these motions can be interpreted as Keplerian circular orbits of hot spots, the astrometric data probe the potential on 8–10 R_g scales (Broderick and Loeb 2006, but see Matsumoto et al. 2020). Combining the strong magnetic field and low density it is then tempting to conclude that the near-face-on orientation of the accretion flow as found by GRAVITY and ALMA reflects the angular momentum of the accretion flow at large distances (Ressler et al. 2018, 2020a). And indeed the observed orientation of the flow deduced from the infrared flares is consistent with the angular momentum

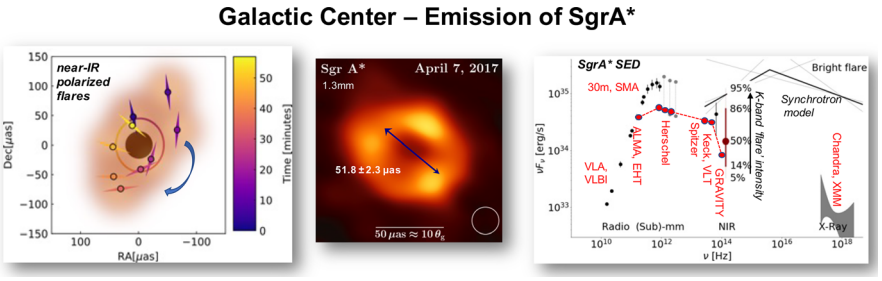

Fig. 4 Evidence for the concentration of the mass of $4.3 \times 10^6 M_\odot$ (as determined from stellar orbits) within few gravitational radii. Left: The flaring NIR emission of SgrA* revolves on a time scale compatible with the Keplerian period at the observed radius. The polarization of the NIR emission rotates on the same time scale. Middle: The EHT-image of SgrA* shows a silhouette as expected for an MBH of $4.3 \times 10^6 M_\odot$. Right: The SED of SgrA*

direction of the 'clockwise' disk of O/WR stars at distances of 1–3″ from SgrA* (GRAVITY Collaboration et al. 2023a). The winds from these stars currently dominate the accretion flow onto SgrA* (Ressler et al. 2020a).

3.4 The Event Horizon Telescope and the detection of the 'shadow' as predicted by GR

The central panel of Fig. 4 shows an image of the compact radio source SgrA* obtained with the 'Event Horizon Telescope', an array of seven telescopes across the globe, and measuring the 1.3 mm continuum radiation of SgrA* (https://eventhorizontelescope.org/, see the more detailed discussion in Fig. 13). The EHT is the pinnacle (in terms of resolution and short wavelength coverage) of the classical radio spatial interferometry Fourier inversion technique (cf. Thompson et al. 2017). Once the collected data are calibrated and analyzed, the EHT can reconstruct the 1.3 mm brightness distribution with a resolution of better than 20 micro-arcsec (Event Horizon Telescope Collaboration et al. 2022a, b). As expected from theory (Sect. 1), the image shows a bright ring with a central dip of diameter 51.8 ± 2.3 micro-arcsec. Given the mass and distance of SgrA* measured with high precision from the stellar orbits (Event Horizon Telescope Collaboration et al. 2022a, b; GRAVITY Collaboration et al. 2023a), GR of a near-face-on accretion zone of moderate to low spin predicts a shadow of diameter 52 ± 0.4 micro-arcsec (Johannsen 2013; Johannsen et al. 2016), in excellent agreement with the EHT measurement (Event Horizon Telescope Collaboration et al. 2022a, b) and a Kerr metric around a 4.3 million solar mass MBH.

The key finding thus is that the *near-event horizon-scale motions from GRAVITY and the size of the 'shadow' of the EHT 1.3 mm emission at 6–9* R_g *are consistent with the GR 'shadow' computed from the prior of mass and distance determined from the stellar orbits at a few* 10^3 R_g. This indicates that any extended mass component within the peri-center motions of the inner most stars is less than a few thousand solar masses (GRAVITY Collaboration et al. 2022b; Will et al. 2023). Both the GRAVITY motions and the EHT size thus constrain the compactness parameter ϵ to be 0.4–0.6, fully consistent with a single MBH in GR (bottom right inset).

The EHT has also detected the predicted shadow in the massive central galaxy of the Virgo galaxy cluster, M87 (or Virgo A) (Event Horizon Telescope Collaboration et al. 2019). The distance of M87 is 16.8 Mpc, 2000 times further away than SgrA*. Since its mass of the central SMBH is 1500 larger than that of SgrA*, $6.2–6.5 \times 10^9\, M_\odot$, the diameter of its shadow is 42 ± 3 micro-arcsec, comparable to that of SgrA*, and strengthening further the 'shadow' interpretation. Detailed polarization images of M87 with the EHT that the near-event horizon magnetic field structure is poloidal and the region is magnetically dominated, as in SgrA* (Event Horizon Telescope Collaboration et al. 2021a, b).

Is there a relativistic jet emanating from SgrA?* Given the strong magnetic field in the accretion zone, and the evidence for a low value of the gas to magnetic pressure, $p(gas)/p(B) \leq 1$ (GRAVITY Collaboration et al. 2018b, 2020c, d, 2023a; Wielgus et al. 2022), one might expect a prominent relativistic radio jet from SgrA*

(Falcke and Markoff 2000). Moreover, if the BH spin were substantial, one would expect that the Blandford and Znajek (1977) mechanism might be effective in accelerating the nuclear spin-driven outflow. Yet, so far, no radio jet feature has been detected, even in relatively high frequency 86 GHz-VLBI maps with exquisite sensitivity (Issaoun et al. 2019), where foreground electron scattering should be less effective in smearing out the jet feature. It is possible that the relative face-on orientation of the central accretion zone would expect the spin to be along the line of sight and thus hard to detect. Alternatively, the SgrA* spin might be low, on the grounds that there is no evidence for strong accretion events in the last few Myrs that could have spun up the MBH (Genzel et al. 2010).

Lack of hard surface? The right panel of Fig. 4 shows the observed radio to X-ray spectral energy distribution of SgrA*, with red labels pointing out the origin of the data (see Genzel et al. 2010; GRAVITY Collaboration et al. 2020a; Falcke and Markoff 2000; Melia and Falcke 2001). The radio to NIR emission exhibits substantial linear polarization, pointing to non-thermal synchrotron emission from the hot accretion flow, as well as possible jet driven outflows. The K- to mid-IR emission is characterized by a semi-continuously variable, linearly polarized source, with a near log-normal flux distribution over 1.5 decades (Genzel et al. 2003; Eckart et al. 2006a, b; Dodds-Eden et al. 2009, 2010, 2011; Do et al. 2009; Witzel et al. 2012, 2018; GRAVITY Collaboration et al. 2020a). The X-ray emission is also highly variable over two orders of magnitude and could come from synchrotron emission as well (Dodds-Eden et al. 2010; Ponti et al. 2017; GRAVITY Collaboration et al. 2021), or, perhaps less likely, from Compton up-scattering of long wavelength photons (Dodds-Eden et al. 2010; Witzel et al. 2021, see also Genzel et al. 2010; Cardoso and Pani 2019). Broderick et al. (2009) have used the relative weakness of the steady infrared emission from the center of SgrA* (< a few percent of the total luminosity of a few 10^{36} erg/s) as an argument in favor of the existence of an event horizon (but Abramowicz et al. 2002; Carballo-Rubio et al. 2023). The basic argument is as follows. Assume matter were accreting onto a hypothetical hard surface outside the gravitational radius, but within the upper limit of $\sim 10R_{\rm g}$ set by the VLBI images. When this accreting matter hits the surface, it will shock, thermalize, and emit all its remaining energy as black-body radiation of a few 10^3 K in the IR range. Such a thermal component is not observed in the steady spectral energy distribution of SgrA* (Genzel et al. 2010; GRAVITY Collaboration et al. 2020a), setting a stringent upper limit on the mass accretion rate. In practice this limit is so low that even the low level of observed quiescent radio/submm nonthermal emission requires an assumed radiative efficiency of nearly 100%. This can be ruled out, which then leads to the conclusion that the central object cannot have a hard surface but rather must have an event horizon ($\epsilon \ll 1$). The caveat is that this consideration does not include gravitational light bending. Lu et al. (2017) make a similar argument on the statistical lack of bright extragalactic tidal disruption events in the Pan-STARRS1 survey.

4 *Allegretto:* GRAVITY measurements of BH masses in distant AGN and quasars

We discussed in Sect. 2 the discovery of quasars 60 years ago, interpreted to be (S) MBHs (10^7 to $10^{10}\,M_\odot$) at large distances, and accreting gas at large rates. Large samples of these active galactic nuclei (AGN, of which quasars are the tip of the iceberg) are now available, all the way back to less than 1 Gyr after the Big Bang, in the Early Universe. In the local Universe the mass of the central MBH and the mass of the central stellar centroid/bulge are about 0.2–0.7% of their host galaxy (Fig. 1 right panel). This correlation suggests that the evolution and growth of the two components are correlated on cosmic time scales (Vestergaard et al. 2008; Vestergaard and Osmer 2009; Alexander and Hickox 2012; Kormendy and Ho 2013; McConnell and Ma 2013; Saglia et al. 2016, and references therein).

How can we test more quantitatively the correctness of the (S)MBH paradigm and the (S)MBH-galaxy co-evolution? 'Type I' AGNs and quasars typically show > few 10^3 km/s line broadening of atomic emission lines by high-velocity motion of gas near the center (Netzer 2013, 2015). If the line widths are due to virialized motions caused by the central mass, and the size of regions for which broad emission lines are observed ('*broad-line regions, BLR*') it then becomes possible to measure the masses of the central (non-stellar) masses in individual AGNs.

One way to estimate the BLR sizes comes from measuring the delay in light travel time between the variable brightness of the accretion disk continuum and the emission lines, a method known as '*reverberation mapping*' (Blandford and McKee 1982). This method has been applied routinely to nearby AGNs (e.g., Kaspi et al. 2000; Bentz et al. 2009, 2010, 2013; Peterson 2014) but is somewhat limited because of the necessary underlying assumptions on the source structure and geometry.

Moreover, ground-based reverberation mapping cannot be easily applied to the very massive, large quasars because of the long time scales involved. Until recently direct imaging of such BLRs has not been possible because of their large distances and resulting small angular size (less than 100 micro-arcsec). For the most distant SMBHs the approach has been to calibrate the relationship between BLR size (inferred from reverberation) and optical luminosity, and then apply the same relationship to higher z SMBH where only line widths and luminosities were available Vestergaard et al. (2008), Vestergaard and Osmer (2009).

The GRAVITY interferometric beam combiner of the 4×8 m telescopes of the ESO-VLT has changed this situation (Fig. 12, GRAVITY Collaboration et al. 2017; GRAVITY+ Collaboration et al. 2022). GRAVITY Collaboration et al. (2018c) were able to resolve the BLR of the famous quasar 3C 273 ($z = 0.16$, 550 Mpc distance, cf. Schmidt 1963) at sub-parsec level with interferometric spectro-astrometry. Figure 6 shows the results. More recently, after incorporating new optics allowing much larger offsets between phase reference star and science object, it has now become possible to apply the same direct technique to faint, distant quasars, such as the quasar J0920 ($z = 2.32$, 17 700 Mpc distance, GRAVITY+ Collaboration et al. 2024; Fig. 5). At this time, there are about a dozen GRAVITY(+) measurements of BLRs (bottom right of Fig. 6).

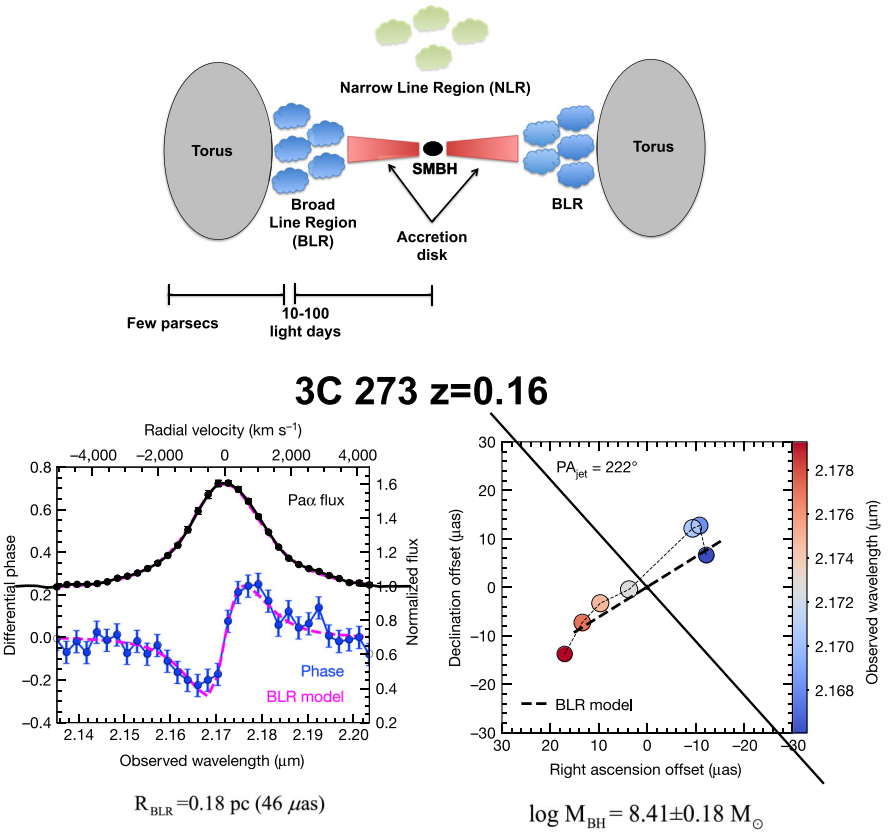

Fig. 5 Top: Schematic of the structures around a luminous, rapidly accreting extragalactic active galactic nucleus ($\dot{M} > 0.01 \times \dot{M}_{\mathrm{max,Eddington}}$), with a super-massive ($> 10^{8...10}\,M_{\odot}$) BH at its center (e.g., Osmer 2004; Netzer 2015). The SMBH is surrounded by a hot accretion disk. Generalizing our current GRAVITY results (Figure 3, GRAVITY Collaboration et al. 2018c; GRAVITY+ Collaboration et al. 2024, and references therein) on its outer side are self-gravitating ionized clouds, the BLR in virial equilibrium and rotating around the SMBH. This central region in turn is surrounded by a dusty molecular region (the "Torus"), and ionized clouds on 100 pc-10 kpc scale (the narrow-line region, NLR). Image credit: Claudio Ricci. Bottom: GRAVITY spectro-astrometry of the broad Pα line in the $z = 0.16$ Quasar 3C 273 (Schmidt 1963). The left panel shows the observed line profile and the inferred interferometric phase gradient across the line, with a measurement accuracy of about 1μas (500 AU, or 0.0024 pc at 550 Mpc distance). The 2D spectro-astrometry model (bottom middle panel) shows that this phase gradient extends over 50 micro-arcsec, approximately perpendicular to the direction of the known radio jet (black line). The model yields a MBH mass of $2.6 \times 10^8\,M_{\odot}$, surrounded by a thick rotating gas disk of 0.18 parsec (46μas) diameter (GRAVITY Collaboration et al. 2018c, cf. Netzer 2020)

Looking ahead at the near-future, the enhanced capabilities of GRAVITY+ will enable measuring super-massive BH masses and their evolution across the entire cosmological evolution of galaxies, and answer the fundamental question whether galaxies, and MBHs grew in lockstep, or whether one of them grew faster and earlier.

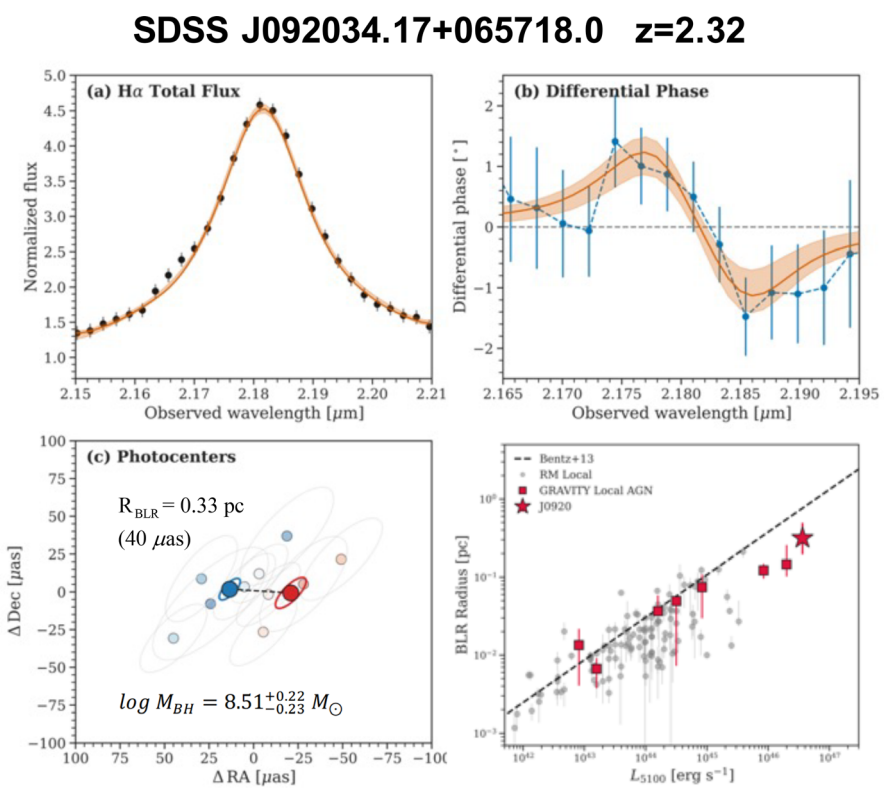

Fig. 6 Top left: GRAVITY spectro-astrometry of the broad Hα line in the $z = 2.32$ quasar J0920, with the new capabilities of 'GRAVITY-wide' to fringe-track on a bright star up to 25″ from the phase center (GRAVITY+ Collaboration et al. 2024). The data and modeling of this distant quasar (distance 17 700 Mpc, 2.89 Gyr after the Big Bang) are qualitatively quite similar to those of the 33 times closer 3C 273, with a linear velocity gradient, indicating predominantly rotation in a 0.33 pc diameter (40 micro-arcsec) thick disk rotating around a $3.2 \times 10^8\, M_\odot$ central mass (top right and bottom left). In contrast to moderately luminous local AGN, 3C 273 and J0920, both optically very luminous (i.e., high Eddington ratio accretion) MBHs, seem to have a smaller broad-line region, and contain a smaller fraction of the overall baryonic mass of the galaxy than predicted by scaling relations (bottom right)

The high-z detections with the new interferometric technique of optically very luminous (i.e., high Eddington ratio accretion) (S)MBHs, may have systematically smaller broad-line regions, and thus contain a smaller (S)MBH mass, than lower Eddington rate AGNs measured in the local Universe with the reverberation technique, and with the velocity-luminosity relations at higher z (bottom right of Fig. 6). Even small shifts as seen here could have big impacts on our understanding of (S)MBH growth as these relations are used to measure masses out to $z = 10$ in usually high luminosity/Eddington quasars and discriminate between black hole seed models.

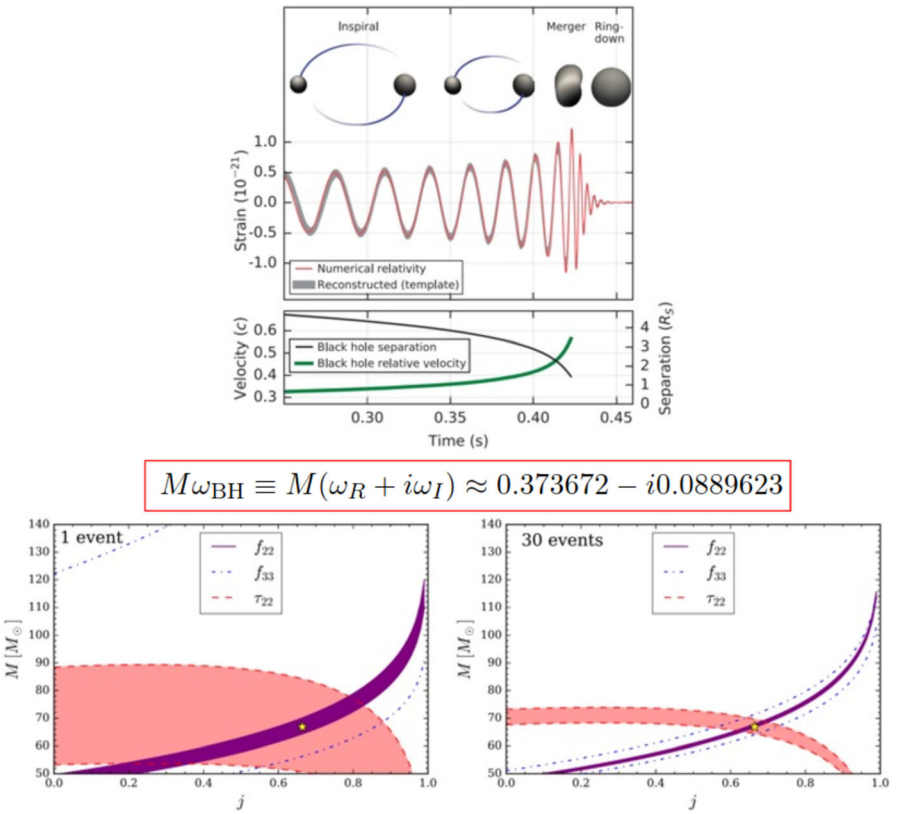

Fig. 7 Top: Inspiral, merger/plunge-in and ring-down of a SBH binary (Abbott et al. 2016a). Bottom: 'Spectroscopy' of a SBH inspiral. Mid and right: The Kerr metric gives a unique relation-ship between mass, and the orbital $l = 2$ mode frequency ω_R near the plunge in, and the imaginary frequency ω_i expressing the decay time of this mode, $t_d \sim 1/\omega_i$ (Cardoso and Pani 2019). Given the short duration of a $2 \times 30\,M_\odot$ inspiral, a single inspiral like GW150914 does not yield enough SNR to determine these frequencies with sufficient accuracy with the current aLIGO sensitivity, and a stacking of about 30 such inspirals would be required (simulation by Brito et al. 2018). The small yellow star is the true input value injected into the simulation

5 *Allegro Molto:* Experimental evidence for stellar BHs from gravitational waves

If two compact stellar masses orbit each other in a tight bound orbit, they lose energy through the emission of gravitational waves. As a result, the orbital semi-major axis shrinks. The inspiral rate is low initially at large orbital radius, but then orbital speed, gravitational wave strain and gravitational wave amplitude increase as the inspiral proceeds. Once the binary has shrunk to the innermost stable orbit, plunge in to a SBH of the combined mass (minus the mass-energy lost due to gravitational wave emission) happens on a dynamical time scale of O (10 milli-sec) or 200 Hz frequency (left panel of Fig. 7). The gravitational strains that need to be detected for successful of binary inspirals lead to pico-meter amplitudes, which can be detected with second

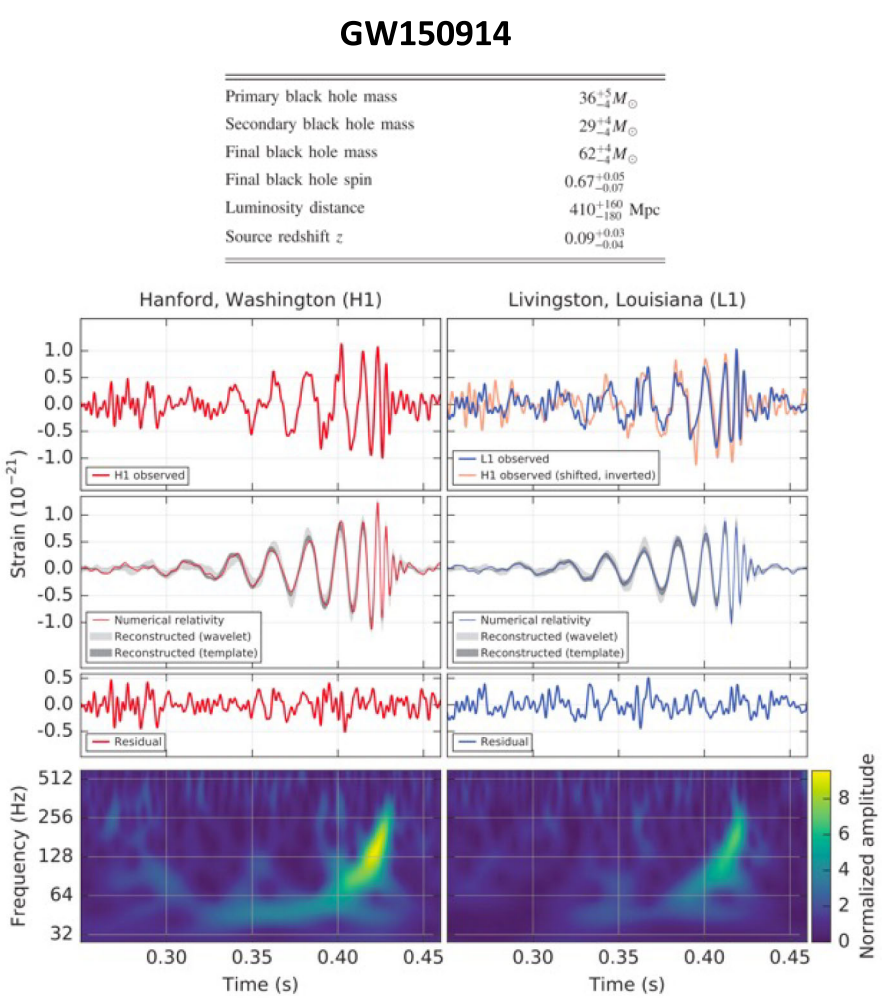

Fig. 8 Data of the first BH-binary inspiral, GW150914, as seen by the Hanford and Livingston antennas of aLIGO, and the derived source properties—Abbott et al. (2016a, 2016b)

and third generation laser-powered Michelson interferometers (https://www.ligo.caltech.edu/, https://gcn.nasa.gov/missions/lvk).

The first spectacular detection was the gravitational-wave pattern from GW150914, with the two gravitational-wave antennas of LIGO in the USA (Abbott et al. 2016a, b). The two initial (S)BHs had masses of about 35 $M_\odot$. Since 2015 and up to the end of the GWTC-3 run, aLIGO, strengthened with the Virgo antenna in Europe, and the KAGRA antenna in Japan, have detected 35 bona fide mergers. These turn out to be SBH-SBH and SBH-NS mergers, but no NS-NS mergers, as well another ~ 50 or so candidate detections (Abbott et al. 2022). This impressive harvest is shown in the in Fig. 9. The data provide very strong, and arguably conclusive evidence for the existence of SBHs.

Starting already with GW150914 (Fig. 8) it perhaps came as a surprise that the SBH masses were larger than expected. According to standard stellar evolution models, the typical SBH in the local Universe is expected to have a mass of $\sim 10\,M_\odot$. While a number of such lower mass inspirals have by now been seen, the relative fraction of $\sim 2 \times 25$–$30\,M_\odot$ objects is fairly, if not uncomfortably, large. Even more surprising is the case of GW190521, with two SBHs of 85 and 66 $M_\odot$ combining to an 'intermediate mass BH' (IMBH) of 142 $M_\odot$ (Abbott et al. 2020). The two initial SBHs of the binary are both in, or near the so called 'pulsational pair instability gap', where the creation of particle-antiparticle pairs during the supernova explosion there prevents a stable SBH mass. While the large fraction of combined mass $\sim 50\,M_\odot$ SBH end states may be explainable by the instrumental sensitivity bias of the current interferometers preferentially selecting larger mass, larger amplitude systems, the case of GW190521 is truly fascinating. Do repeated mergers in dense star clusters explain the large masses, or is there a new, yet unknown channel of massive SBH and IMBH creation?

Black-hole spectroscopy It is clear that the largest information about the space-time and significant tests of the no-hair theorem can in principle obtained in the last, near-event horizon inspirals, before plunge in. In technical terms this 'BH spectroscopy' requires accurate determination of the near-photon orbit, orbital frequency and its decay time (Brito et al. 2018; Berti et al. 2018; Cardoso and Pani 2019; Fig. 7). The Kerr metric specifies a precise relation between the $l = 2$ mode 'normal' frequency (at the photon orbit), and the decay time (Fig. 7). The frequency analysis of the GW150914 ring down (the strongest and highest quality inspiral as of today) is consistent with Fig. 7 in the $l = 2$ mode, and thus with the Kerr metric (Abbott et al. 2016b). However, (Brito et al. 2018, bottom panels of Fig. 7) have

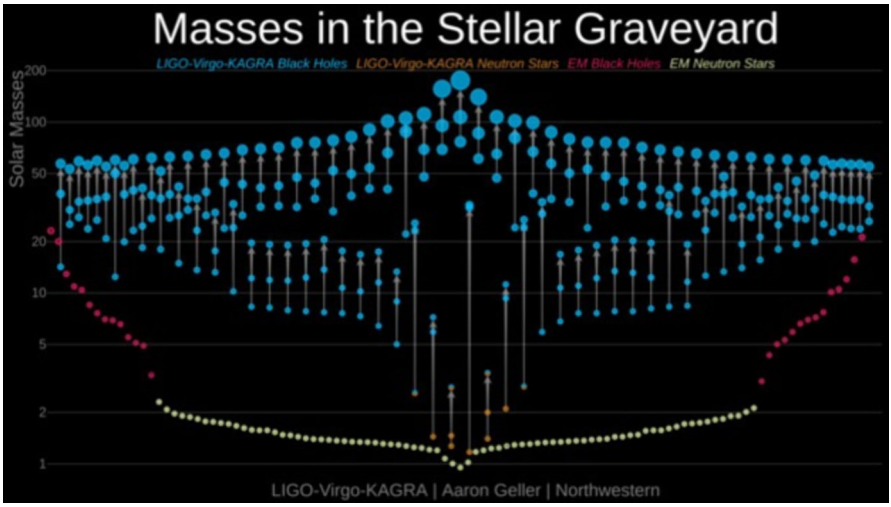

Fig. 9 Current status of the SBH-SBH and SBH-NS inspirals observed by aLIGO and aLIGO+Virgo+KAGRA after GWTC-3 (Fig. 14, right panel, Abbott et al. 2016a, b, 2022). Compilation of the inferred inspiral masses of all events seen at the end of the GWTC-3 run with LIGO, Virgo and KAGRA Abbott et al. (2023). Image courtesy of https://www.ligo.caltech.edu/image/ligo20211107a

shown that a full test of the no-hair theorem requires also the determination of the frequencies and decay times of the $l > 2$ modes, which is not yet possible with one inspiral. They estimate that about 30 inspirals need to be combined to achieve that test. However, there is very good hope that the ground-based interferometer of the next generation and the space interferometer LISA will make dramatic improvements (Fig. 9).

6 *Rondo:* Dark matter cusps

Viollier et al. (1993) and Munyaneza et al. (1999) proposed that the dark matter concentrations in galactic nuclei, including QSOs, may not be Kerr BHs, but very compact '*fermion balls*' (for example made of hypothetical, massive neutrinos) supported by degeneracy pressure. The size of a fermion ball, and the maximum stable 'Chandrasekhar' mass (or its relativistic analog, the 'Oppenheimer–Volkoff' mass $M_{\rm OV}$, Oppenheimer and Snyder 1939), increase the lighter the fermion's mass. In this scenario the largest observed central masses in elliptical galaxies, a few $10^{10}\,M_\odot$, would approach the Oppenheimer–Volkoff mass, resulting in an upper limit to the mass of the constituent fermions to about $13\,\mathrm{keV/c^2}$, again with larger BH masses requiring smaller neutrino masses. To still 'fit' within a given peri-center distance the neutrinos would have to have a mass of Munyaneza et al. (1999)

$$m_{\rm f} \sim 70\,\mathrm{keV\,c^{-2}} \left(\frac{\mathrm{R_{peri}}}{10\,\mathrm{light\ hours}}\right)^{-3/8} \left(\frac{\mathrm{g}}{2}\right)^{-1/4} \left(\frac{\mathrm{M_{OV}}}{4.4\times10^6\,\mathrm{M_\odot}}\right)^{-1/8} \tag{3}$$

where g is the spin degeneracy factor of the fermion.

Ruffini et al. (2015) and Argüelles et al. (2019) have pointed out that a self-gravitating equilibrium distribution of massive neutral fermions of given degeneracy g exhibits a segregation into three physical regimes. There is an inner core of almost constant density governed by degenerate quantum statistics. Surrounding this core is an intermediate region with a sharply decreasing density distribution, which in turn is

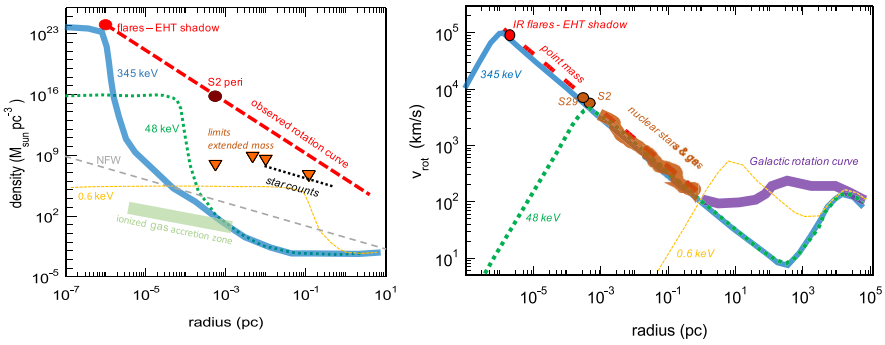

Fig. 10 Constraints on the contribution of various mass components of baryonic and dark fermionic matter (fermion ball) to the central mass density (left) and rotation velocity (right) at different radii R (adapted from Argüelles et al. 2019, 2023)

surrounded by an extended plateau. Finally, there is an outer, asymptotic halo where density scales as $\rho \propto R^{-2}$, i.e., a classical Boltzmann regime (Fig. 10, adapted from Argüelles et al. 2019, 2023. The Ruffini et al. (2015) model unifies dark matter on large, intergalactic and circum-galactic scales, with the evidence of central massive concentrations discussed in Sects. 2–5. The Boltzmann distribution would explain the flat rotation curves on $\gg$10 kpc scales, while baryons in form of gas and stars would explain the mid-scales (parsec to 10+ kpc). Figure 10 shows the resulting density distributions and rotation curve distributions as a function of radius, for three different 'fermions', of $m_{\rm f} = 0.6$, 48 and 345 keV. As pointed out above, for a given fermion mass $m_{\rm f}$ in Eq. (3), $M_{\rm OV}$ gives the critical stable mass, above which gravity will take over and the object collapses (to a (S)MBH). Likewise, if there is substantial baryonic accretion onto such a dark matter core, the central mass concentration would also collapse to a (S)MBH (Argüelles et al. 2024).

Figure 10 summarizes the current constraints on the fermion ball, or fermion-dark matter model in the Galactic Center. The outer flat rotation curve of the Galaxy would be best matched by moderate mass, 10–50 keV fermions (Argüelles et al. 2019, 2023; Becerra-Vergara et al. 2021). The nuclear stellar and gas velocities (GRAVITY Collaboration et al. 2022b) are in principle also consistent with a 40+ keV dark matter core (Becerra-Vergara et al. 2020, 2021; Argüelles et al. 2023). However, the excellent agreement of the measured prograde precession of S2 at $R_{\rm peri} = 5.7 \times 10^{-4}$ pc with that expected for a MBH GRAVITY Collaboration et al. (2020c, 2022b) is barely consistent with such a lower mass dark matter particle. There is also a modest inconsistency with the density of ionized baryonic mass estimated at a few $10^3\, R_{\rm g}$ (Gillessen et al. 2019).

If the infrared flare motions ($\sim 0.28c$ on the sky at 8–9 $R_{\rm g}$, GRAVITY Collaboration et al. 2018b, 2023a) represent the Keplerian orbital speed, and the EHT shadow diameter Event Horizon Telescope Collaboration et al. (2022a, 2022b) is a measure of the light bending by a central mass, then the implied fermion mass would have to be $\sim$500 keV, obviously very close to the MBH solution. Such a large fermion mass is disfavored for the favored dark matter agent on large scales Argüelles et al. (2023). It would also be inconsistent with the mass densities inferred from the BLR in AGN and quasars (see Sect. 4).

Another proposed non-BH configuration is the '*boson star*' scenario advanced by Torres et al. (2000). A wide range of boson star masses can theoretically be imagined, including ones with masses of (S)MBHs, depending on the assumptions about the specific boson particle masses and their self-interactions. Since such an object consists of weakly interacting particles it is unclear how it may have formed. The size of a boson star is only a few times $R_{\rm S}$ of the same mass (S)MBH, and is highly relativistic. It is clear from Fig. 10 that even the astrometric observations of the IR flares are not sufficient to distinguish a boson star from a MBH in the Galactic Center (Rosa et al. 2022). The motion of test-particles crossing the boson star would allow to distinguish boson stars from BHs (Zhang et al. 2022), but are currently far out of reach. The EHT imagery is more promising. Ray-tracing simulations by Vincent et al. (2016) and Olivares et al. (2020) suggest that the mm-appearance of an accreting boson star can be close to that of a MBH, although 'ideal' cases with a

large shadow as seen in the Galactic Center, or M87 Event Horizon Telescope Collaboration et al. (2022a, 2022b, 2019) are rare. More detailed EHT observations are likely to separate in more detail the time variable, from the stationary parts of the shadow, thus helping to distinguish between the MBH and boson star cases.

Finally, Occam's razor strongly disfavors the boson star interpretation for rapidly accreting AGNs/quasars. A boson star obviously is unstable to collapse to a BH if it experiences substantial baryonic accretion. While this is not the case in the Galactic Center currently, such high Eddington ratio events almost certainly happened in the evolution of most, and perhaps all, (S)MBHs.

Classical (particle-like) dark matter models predict that dark matter will cluster around the massive black holes in galaxy centers (Gondolo and Silk 1999; Sadeghian et al. 2013). In principle, such dark matter spikes could have high enough densities to affect the motions of objects around the MBH (Zakharov et al. 2007; Lacroix 2018). Yet, the detection of dark matter in that way might be impossible, due to the expected background population of dark objects such as white dwarfs, neutron stars and stellar black holes, that should arrange into a spiky distribution centered on the MBH (Merritt 2010; Antonini 2014; Linial and Sari 2022), and that simply might outweigh the dark matter particles. Current limits from GRAVITY observations stand at around $4000\,M_\odot$ (GRAVITY Collaboration et al. 2022b).

7 *Coda Fortissimo:* Future expectations for studying astrophysical BHs

A century after the publication of Einstein's field equations and Schwarzschild's first solution (Einstein 1916; Schwarzschild 1916), 60 years after the Kerr/Newman (1963–65) solutions, and the discovery of X-ray binaries (Giacconi et al. 1962) and quasars (Schmidt 1963), BHs have come from theoretical speculation to near experimental certainty. The recent progress in electromagnetic and gravitational wave studies has been truly remarkable, the top experiments (VLT-GRAVITY-Keck, EHT, aLIGO-Virgo-KAGRA) have been a tour de force of experimental physics, and the experimental work and scientific results have been recognized with two Nobel Prizes, and several Balzan, Shaw, Gruber and Breakthrough Prizes so far.

Yet let us stay realistic and humble. Measured on the expectation level of critical theoretical colleagues, and certainly on the ultimate requirement for establishing 'scientific truth', *the evidence we currently have is impressive on all accounts but not (yet fully) conclusive*. We have constrained the ϵ-parameter to a few tenths, leaving in principle open the possibility that the objects we have been studying are not BHs after all but speculative ECOs, such as fermion or boson stars, gravastars, wormholes etc. (see Sect. 6, and the detailed review of Cardoso and Pani 2019). It is also possible that GR is not the correct description of space time close to the event horizon (cf. Cardoso and Pani 2019 and references therein).

In Fig. 11 below we have listed where we currently stand, and where we might get to in the next decades, for proving the MBH paradigm in terms of the compactness parameter, or equivalently the no-hair theorem test, with the parameter $\epsilon = 0$ for a Kerr hole.

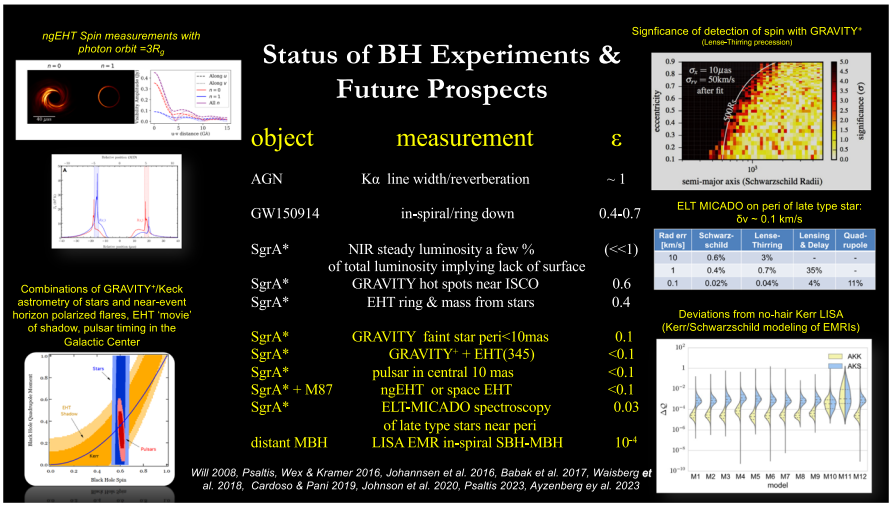

Fig. 11 Current status and future improvements in the quality of experimental studies of the BH paradigm. The central table lists the constraints (here in the compactness parameter ϵ, where $\epsilon = 0$ is a Kerr BH) achieved so far by the different techniques discussed in the text are in white color, while the expected further improvements in the future are in yellow. Current state of the art sets limits in ϵ of a few tenths. The very faint stationary near-infrared emission of SgrA* can in principle be interpreted as a strong evidence for the absence of a surface of the source, and thus in favor of an event horizon. However, this argument relies on the emission be isotropic and not strongly affected by gravitational lensing. Detection with GRAVITY+ of the Lense–Thirring precession of a star with $R_{\rm peri} < 10$ μas would yield a spin determination of the MBH in the Galactic Center, and together with other stars yield a limit of $\epsilon \sim 0.1$. Higher quality measurements of the photon-ring ($n \geq 1$) in SgrA* with ngEHT, or space VLBI (together with the priors from GRAVITY+ would reach $\epsilon < 0.1$. The same limit could be reached with timing of a Galactic Center pulsar within an arcsecond of SgrA*. Still better limits could then come from a combination of all three techniques in the next 10 years. Detailed 100 m/s spectroscopy with MICADO@ELT in the 2030s of a late type star in a close peri-approach to SgrA* might achieve $\epsilon \sim 0.03$. Finally gravitational wave analysis of an inspiral of a stellar BH into a MBH (EMRI) would reach $\epsilon \sim 0.0001$ with LISA data in 2+ decades

It is clear that the best LIGO-Virgo-KAGRA SBH inspirals already set ϵ significantly below unity, likewise so for the most recent combination of stellar, flare and EHT-shadow data. If GRAVITY+ can measure a high quality orbit of a star with a peri-center distance 2–4 times smaller than S2, or if one can determine the pulse timing of a sufficiently nearby pulsar, or the combination of GRAVITY+ and EHT (including possible upgrades in performance), the next step is $\epsilon \leq 0.1$, allowing spin measurements (Waisberg et al. 2018) and no-hair theorem tests (Falcke et al. 2000; Will 2008; Psaltis and Johannsen 2011; Psaltis et al. 2016; Johannsen 2016; Johnson et al. 2020, lower top panel of Fig. 6). The enormously greater sensitivity of MICADO at the ESO-ELT could push the spectroscopic measurement precision in 5–10 years to m/s level (Davies et al. 2021). For a late-type star near peri-center that could push to $\epsilon \sim 0.03$. Future extensions of the VLTI to a kilometer-wide interferometric array could push the angular resolution to better than 100 micro-arcsecond and astrometry to sub-micro-arcsec precision, thereby opening up the observation of the scattering of S-stars by neutron stars and stellar black holes, and

spatially resolving the accretion zone and flaring activity at IR wavelengths. An expanded ground-based mm-/submm-VLBI network, such as the ngEHT (Ayzenberg et al. 2024) could test the space-time at the photon-orbit. The European ELT and GRAVITY+ will also probe the formation and evolution of the first SMBHs, such as the JWST source GN–z11 at $z = 10.6$ (Maiolino et al. 2024; Schneider et al. 2023).

An important question is, how far the measurement accuracy of the small higher order PPN-terms can be pushed before perturbations with other stars and SBHs introduce 'orbital chaos' that diminishes or even wipes out the GR information and significant tests of the no-hair theorem. Merritt et al. (2010) carried out a suite of simulations and concluded that in the dense region around the MBH the perturbations indeed are likely too strong to measure the Lense–Thirring precession. However, the work of Merritt et al. (2010) only considered orbit averaged quantities and assumed an overly high density of SBHs in the central region, which the current limits on any extended mass around SgrA* now show to be far too large. Moreover, we now know that many of the S-stars are on highly elliptical orbits and spend little time in the high density region around the MBH. The perturbative 'chaos' thus is dominated by single star-star and star-SBH events, when the three are near peri-approach. Portegies Zwart et al. (2023) have studied this 'punctuated chaos' with high quality N-body integrations of the known S-star orbits. When two S-stars come very close (a few tens of AU) during peri of 100–1000 AU, they indeed experience exponential growth of the orbital deviations in their separation in parameter space. Still the average exponential growth time, the Lyapunov time, is 460 years. This is encouraging if indeed faint stars of <100 AU peri-distance occur that in principle allow measurements of the Lense–Thirring and quadrupole terms (Waisberg et al. 2018).

On a time scale of 20 years, the gravitational-wave mission LISA of ESA should deliver the ultimate test. This space interferometer with three satellites forming a laser interferometer of 2.5 million km length is sensitive to gravitational waves with 4–5 orders lower frequency, and thus correspondingly larger masses (Amaro-Seoane et al. 2023; Colpi et al. 2024). LISA will be able to observe the inspirals of MBHs across the entire Universe (Barausse et al. 2020). The inspiral of a SBH into a MBH (an extreme mass ratio inspiral, EMRI: Amaro-Seoane et al. 2017; Amaro-Seoane 2019) should deliver enough SNR in the inspiral before plunge, to obtain a high-quality measurements of the fundamental ($l = 2$) quasi-normal mode of the MBH at the photon orbit, and get to $\epsilon \sim 10^{-4}...10^{-3}$ (Buonanno et al. 2007; Babak et al. 2017; Cardoso and Pani 2019). This would provide the ultimate culmination of this exciting journey, which Albert Einstein started more than a century ago.

Appendix: Instrumental techniques

All three experimental approaches discussed in this review apply variations of the interference of light in a two-beam Michelson interferometer (Michelson and Morley 1887).

GRAVITY Figure 12 summarizes the essentials of the stellar interferometry at 2μm (K-band) with the GRAVITY(+) beam combiner at the ESO VLTI (GRAVITY Collaboration et al. 2017; Eisenhauer et al. 2023, https://www.mpe.mpg.de/ir/gravity, https://www.mpe.mpg.de/ir/gravityplus). GRAVITY coherently combines the light from the four 8 m UT or 1.8 m AT telescopes (left bottom). Each telescope is equipped with adaptive optics to provide a diffraction-limited beam, which is then transported through mirrored delay lines to the cryogenic beam combiner instrument (right top). The instrument provides two beam combiners, one for fringe tracking, the other optimized for long exposure, high spectral resolution interferometry of the science target. The optical path length within the observatory is controlled via several laser metrology systems, delay lines, and differential delay lines (top).

Event Horizon Telescope The Event Horizon Telescope (EHT) is a further development of the technique of intercontinental, heterodyne stellar interferometry (Thompson et al. 2017) pushed to the highest microwave frequencies (230/345 GHz), at which the Earth Atmosphere is still transparent. The Very Large Baseline Interferometry (Event Horizon Telescope Collaboration et al. 2022a, https://eventhorizontelescope.org/, https://blackholecam.org/) links radio telescopes across the globe to create an Earth sized interferometer (left panel in Fig. 13). Both

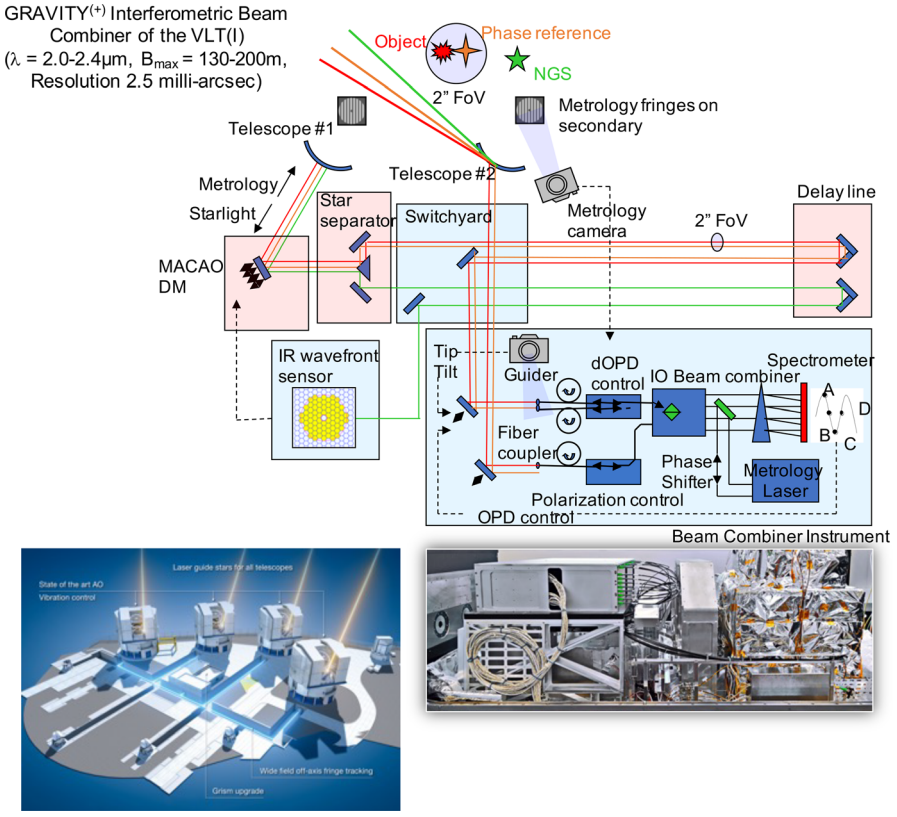

Fig. 12 GRAVITY. See text. Image credits: ESO/GRAVITY(+) collaborations

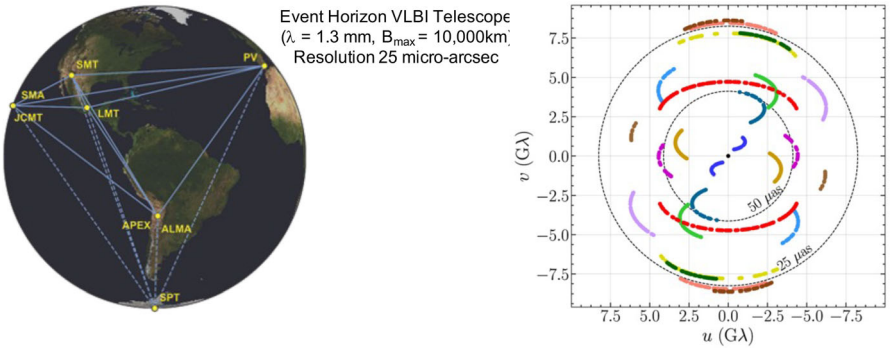

Fig. 13 Event Horizon Telescope. See text. Image credits: EHT collaboration

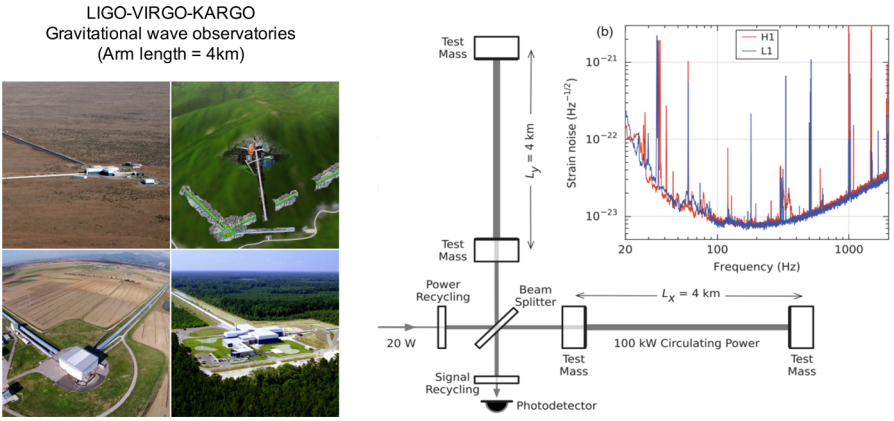

Fig. 14 Ground-based gravitational-wave interferometry. See text. Image credits: LIGO/Virgo/KAGRA collaborations

techniques—optical/IR and radio interferometery—synthesize a virtual telescope of diameter $B_{\max}$ (the maximum separation between two telescopes in the array) with an angular resolution $\lambda/B_{\max}$. They measure the Fourier components of the image at the projected separation of the telescopes (right).

Ground-based gravitational-wave interferometry Figure 14 summarizes the essentials of ground-based gravitational wave, laser interferometry, and in particular the LIGO, Virgo, KAGRA gravitational-wave observatories (Abbott et al. 2016a, https://www.ligo.caltech.edu/, https://gcn.nasa.gov/missions/lvk). The experiments measure the small distortions of space-time when gravitational waves pass through the two arms of the interferometer (right). In this case one of the two arms will be stretched, while the other arm shortened. Ground-based gravitational-wave detectors are most sensitive at frequency of 20 to several hundred Hz (inset), which matches the orbital frequencies of stellar black-hole mergers.

Acknowledgements The authors are grateful to the numerous contributions from GRAVITY team members in Germany, France, and Portugal, as well as the generous support from ESO and their staff,

including the entire Paranal Observatory. None of the relevant research discussed in this review would have been possible without this fantastic team spirit and the key technical and scientific inputs from all our colleagues. We are grateful to Vitor Cardoso, Thibault Damour, Hagai Netzer, Diogo Ribeiro, Taro Shimizu, and our Editor, P.T.P. Ho, for helpful comments on the text.

Funding Open Access funding enabled and organized by Projekt DEAL.

References

Abbott BP, Abbott R, Abbott TD et al (2016a) GW151226: observation of gravitational waves from a 22-solar-mass binary black hole coalescence. Phys Rev Lett 116(24):241103. https://doi.org/10.1103/PhysRevLett.116.241103. arXiv:1606.04855 [gr-qc]

Abbott BP, Abbott R, Abbott TD et al (2016b) Astrophysical implications of the binary black-hole merger GW150914. ApJ 818(2):L22. https://doi.org/10.3847/2041-8205/818/2/L22. arXiv:1602.03846 [astro-ph.HE]

Abbott R, Abbott TD, Abraham S et al (2020) Properties and astrophysical implications of the 150 $M_{\odot}$ binary black hole Merger GW190521. ApJ 900(1):L13. https://doi.org/10.3847/2041-8213/aba493. arXiv:2009.01190 [astro-ph.HE]

Abbott R, Abbott TD, Acernese F et al (2022) Search for intermediate-mass black hole binaries in the third observing run of advanced LIGO and advanced Virgo. A&A 659:A84. https://doi.org/10.1051/0004-6361/202141452. arXiv:2105.15120 [astro-ph.HE]

Abbott R, Abbott TD, Acernese F et al (2023) Population of merging compact binaries inferred using gravitational waves through GWTC-3. Phys Rev X 13(1):011048. https://doi.org/10.1103/PhysRevX.13.011048. arXiv:2111.03634 [astro-ph.HE]

Abramowicz MA, Kluźniak W, Lasota JP (2002) No observational proof of the black-hole event-horizon. A&A 396:L31–L34. https://doi.org/10.1051/0004-6361:20021645. arXiv:astro-ph/0207270

Alexander T (2005) Stellar processes near the massive black hole in the Galactic center [review article]. Phys Rep 419(2–3):65–142. https://doi.org/10.1016/j.physrep.2005.08.002. arXiv:astro-ph/0508106

Alexander T (2017) Stellar dynamics and stellar phenomena near a massive black hole. ARA&A 55(1):17–57. https://doi.org/10.1146/annurev-astro-091916-055306. arXiv:1701.04762 [astro-ph.GA]

Alexander DM, Hickox RC (2012) What drives the growth of black holes? New A Rev 56(4):93–121. https://doi.org/10.1016/j.newar.2011.11.003. arXiv:1112.1949 [astro-ph.GA]

Almheiri A, Marolf D, Polchinski J et al (2013) Black holes: complementarity or firewalls? J High Energy Phys 2013:62. https://doi.org/10.1007/JHEP02(2013)062. arXiv:1207.3123 [hep-th]

Amaro-Seoane P (2019) Extremely large mass-ratio inspirals. Phys Rev D 99(12):123025. https://doi.org/10.1103/PhysRevD.99.123025. arXiv:1903.10871 [astro-ph.GA]

Amaro-Seoane P, Audley H, Babak S, et al (2017) Laser Interferometer Space Antenna. arXiv e-prints arXiv:1702.00786 [astro-ph.IM]

Amaro-Seoane P, Andrews J, Arca Sedda M et al (2023) Astrophysics with the Laser Interferometer Space Antenna. Living Rev Relativ 26:2. https://doi.org/10.1007/s41114-022-00041-y. arXiv:2203.06016 [gr-qc]

Antonini F (2014) On the distribution of stellar remnants around massive black holes: slow mass segregation, star cluster inspirals, and correlated orbits. ApJ 794(2):106. https://doi.org/10.1088/0004-637X/794/2/106. arXiv:1402.4865 [astro-ph.GA]

Argüelles CR, Krut A, Rueda JA et al (2019) Can fermionic dark matter mimic supermassive black holes? Int J Mod Phys D 28(14):1943003. https://doi.org/10.1142/S021827181943003X. arXiv:1905.09776 [astro-ph.GA]

Argüelles CR, Becerra-Vergara EA, Rueda JA et al (2023) Fermionic dark matter: physics, astrophysics, and cosmology. Universe 9(4):197. https://doi.org/10.3390/universe9040197. arXiv:2304.06329 [astro-ph.GA]

Argüelles CR, Rueda JA, Ruffini R (2024) Baryon-induced collapse of dark matter cores into supermassive black holes. ApJ 961(1):L10. https://doi.org/10.3847/2041-8213/ad1490. arXiv:2312.07461 [astro-ph.GA]

Arkani-Hamed N, Dimopoulos S, Dvali G (1998) The hierarchy problem and new dimensions at a millimeter. Phys Lett B 429(3):263–272. https://doi.org/10.1016/S0370-2693(98)00466-3

Ayzenberg D, Blackburn L, Brito R, et al (2024) Fundamental physics opportunities with the next-generation event horizon telescope. Living Rev Relativ 27. arXiv:2312.02130 [astro-ph.HE]

Babak S, Gair J, Sesana A et al (2017) Science with the space-based interferometer LISA. V. Extreme mass-ratio inspirals. Phys Rev D 95(10):103012. https://doi.org/10.1103/PhysRevD.95.103012. arXiv:1703.09722 [gr-qc]

Baganoff FK, Maeda Y, Morris M et al (2003) Chandra X-ray spectroscopic imaging of Sagittarius A* and the central parsec of the galaxy. ApJ 591(2):891–915. https://doi.org/10.1086/375145. arXiv:astro-ph/0102151

Barausse E, Berti E, Hertog T et al (2020) Prospects for fundamental physics with LISA. Gen Relativ Gravit 52(8):81. https://doi.org/10.1007/s10714-020-02691-1. arXiv:2001.09793 [gr-qc]

Bardeen JM (1973) Timelike and null geodesics in the Kerr metric. Black holes (Les Astres Occlus). Gordon and Breach, New York, pp 215–239

Bardeen JM, Press WH, Teukolsky SA (1972) Rotating black holes: locally nonrotating frames, energy extraction, and scalar synchrotron radiation. ApJ 178:347–370. https://doi.org/10.1086/151796

Bardeen JM, Carter B, Hawking SW (1973) The four laws of black hole mechanics. Commun Math Phys 31(2):161–170. https://doi.org/10.1007/BF01645742

Becerra-Vergara EA, Argüelles CR, Krut A et al (2020) Geodesic motion of S2 and G2 as a test of the fermionic dark matter nature of our Galactic core. A&A 641:A34. https://doi.org/10.1051/0004-6361/201935990. arXiv:2007.11478 [astro-ph.GA]

Becerra-Vergara EA, Argüelles CR, Krut A et al (2021) Hinting a dark matter nature of Sgr A* via the S-stars. MNRAS 505(1):L64–L68. https://doi.org/10.1093/mnrasl/slab051. arXiv:2105.06301 [astro-ph.GA]

Becklin EE, Gatley I, Werner MW (1982) Far-infrared observations of Sagittarius A: the luminosity and dust density in the central parsec of the galaxy. ApJ 258:135–142. https://doi.org/10.1086/160060

Bekenstein JD (1975) Statistical black-hole thermodynamics. Phys. Rev. D 12(10):3077–3085. https://doi.org/10.1103/PhysRevD.12.3077

Bentz MC, Peterson BM, Netzer H et al (2009) The radius-luminosity relationship for active galactic nuclei: the effect of host-galaxy starlight on luminosity measurements. II. The full sample of reverberation-mapped AGNs. ApJ 697(1):160–181. https://doi.org/10.1088/0004-637X/697/1/160. arXiv:0812.2283 [astro-ph]

Bentz MC, Walsh JL, Barth AJ et al (2010) The lick AGN monitoring project: reverberation mapping of optical hydrogen and helium recombination lines. ApJ 716(2):993–1011. https://doi.org/10.1088/0004-637X/716/2/993. arXiv:1004.2922 [astro-ph.CO]

Bentz MC, Denney KD, Grier CJ et al (2013) The low-luminosity end of the radius-luminosity relationship for active galactic nuclei. ApJ 767(2):149. https://doi.org/10.1088/0004-637X/767/2/149. arXiv:1303.1742 [astro-ph.CO]

Berti E, Yagi K, Yunes N (2018) Extreme gravity tests with gravitational waves from compact binary coalescences: (I) inspiral-merger. Gen Relativ Gravit 50(4):46. https://doi.org/10.1007/s10714-018-2362-8. arXiv:1801.03208 [gr-qc]

Blandford RD (1999) Relativistic accretion. In: Sellwood JA, Goodman J (eds) Astrophysical Discs—an EC summer school, ASP conference series, vol 160. Astronomical Society of the Pacific, pp 265. arXiv:astro-ph/9902001

Blandford RD, Begelman MC (1999) On the fate of gas accreting at a low rate on to a black hole. MNRAS 303(1):L1–L5. https://doi.org/10.1046/j.1365-8711.1999.02358.x. arXiv:astro-ph/9809083
Blandford RD, McKee CF (1982) Reverberation mapping of the emission line regions of Seyfert galaxies and quasars. ApJ 255:419–439. https://doi.org/10.1086/159843
Blandford RD, Znajek RL (1977) Electromagnetic extraction of energy from Kerr black holes. MNRAS 179:433–456. https://doi.org/10.1093/mnras/179.3.433
Blandford R, Meier D, Readhead A (2019) Relativistic jets from active galactic nuclei. ARA&A 57:467–509. https://doi.org/10.1146/annurev-astro-081817-051948. arXiv:1812.06025 [astro-ph.HE]
Boehle A, Ghez AM, Schödel R et al (2016) An improved distance and mass estimate for Sgr A* from a multistar orbit analysis. ApJ 830(1):17. https://doi.org/10.3847/0004-637X/830/1/17. arXiv:1607.05726 [astro-ph.GA]
Bousso R (2002) The holographic principle. Rev Mod Phys 74(3):825–874. https://doi.org/10.1103/RevModPhys.74.825. arXiv:3020.3101 [hep-th]
Bower GC, Broderick A, Dexter J et al (2018) ALMA polarimetry of Sgr A*: probing the accretion flow from the event horizon to the bondi radius. ApJ 868(2):101. https://doi.org/10.3847/1538-4357/aae983. arXiv:1810.07317 [astro-ph.HE]
Brito R, Buonanno A, Raymond V (2018) Black-hole spectroscopy by making full use of gravitational-wave modeling. Phys. Rev. D 98(8):084038. https://doi.org/10.1103/PhysRevD.98.084038. arXiv:1805.00293 [gr-qc]
Broderick AE, Loeb A (2006) Imaging optically-thin hotspots near the black hole horizon of Sgr A* at radio and near-infrared wavelengths. MNRAS 367(3):905–916. https://doi.org/10.1111/j.1365-2966.2006.10152.x. arXiv:astro-ph/0509237
Broderick AE, Loeb A, Narayan R (2009) The event horizon of Sagittarius A*. ApJ 701(2):1357–1366. https://doi.org/10.1088/0004-637X/701/2/1357. arXiv:0903.1105 [astro-ph.HE]
Buonanno A, Cook GB, Pretorius F (2007) Inspiral, merger, and ring-down of equal-mass black-hole binaries. Phys. Rev. D 75(12):124018. https://doi.org/10.1103/PhysRevD.75.124018. arXiv:gr-qc/0610122
Carballo-Rubio R, Filippo FD, Liberati S et al (2023) Constraints on thermalizing surfaces from infrared observations of supermassive black holes. J Cosmol Astropart Phys 11:041. https://doi.org/10.1088/1475-7516/2023/11/041. arXiv:2306.17480 [astro-ph.HE]
Cardoso V, Pani P (2019) Testing the nature of dark compact objects: a status report. Living Rev Relativ 22:4. https://doi.org/10.1007/s41114-019-0020-4. arXiv:1904.05363 [gr-qc]
Carr BJ (1975) The primordial black hole mass spectrum. ApJ 201:1–19. https://doi.org/10.1086/153853
Carr BJ, Hawking SW (1974) Black holes in the early Universe. MNRAS 168:399–416. https://doi.org/10.1093/mnras/168.2.399
Carter B (1971) Axisymmetric black hole has only two degrees of freedom. Phys Rev Lett 26(6):331–333. https://doi.org/10.1103/PhysRevLett.26.331
Collaboration Event Horizon Telescope, Akiyama K, Alberdi A et al (2019) First M87 event horizon telescope results. I. The shadow of the supermassive black hole. ApJ 875(1):L1. https://doi.org/10.3847/2041-8213/ab0ec7. arXiv:1906.11238 [astro-ph.GA]
Colpi M, Danzmann K, Hewitson M, et al (2024) LISA definition study report. arXiv e-prints arXiv:2402.07571 [astro-ph.CO]
Crawford MK, Genzel R, Harris AI et al (1985) Mass distribution in the galactic centre. Nature 315(6019):467–470. https://doi.org/10.1038/315467a0
Christodoulou D (1970) Reversible and irreversible transformations in black-hole physics. Phys Rev Lett 25:1596–1597. https://doi.org/10.1103/PhysRevLett.25
Christodoulou D, Ruffini R (1971) Reversible transformations of a charged black hole. Phys Rev D 4(12):3552–3555. https://doi.org/10.1103/PhysRevD.4.3552
Davies R, Hörmann V, Rabien S et al (2021) MICADO: the multi-adaptive optics camera for deep observations. Messenger 182:17–21. https://doi.org/10.18727/0722-6691/5217. arXiv:2103.11631 [astro-ph.IM]
Dexter J, Tchekhovskoy A, Jiménez-Rosales A et al (2020) Sgr A* near-infrared flares from reconnection events in a magnetically arrested disc. MNRAS 497(4):4999–5007. https://doi.org/10.1093/mnras/staa2288. arXiv:2006.03657 [astro-ph.HE]
Do T, Ghez AM, Morris MR et al (2009) A near-infrared variability study of the galactic black hole: a red noise source with no detected periodicity. ApJ 691(2):1021–1034. https://doi.org/10.1088/0004-637X/691/2/1021. arXiv:0810.0446 [astro-ph]

Do T, Hees A, Ghez A et al (2019a) Relativistic redshift of the star S0-2 orbiting the Galactic Center supermassive black hole. Science 365(6454):664–668. https://doi.org/10.1126/science.aav8137. arXiv:1907.10731 [astro-ph.GA]

Do T, Witzel G, Gautam AK et al (2019b) Unprecedented near-infrared brightness and variability of Sgr A*. ApJ 882(2):L27. https://doi.org/10.3847/2041-8213/ab38c3. arXiv:1908.01777 [astro-ph.GA]

Dodds-Eden K, Porquet D, Trap G et al (2009) Evidence for X-ray synchrotron emission from simultaneous mid-infrared to X-ray observations of a strong Sgr A* flare. ApJ 698(1):676–692. https://doi.org/10.1088/0004-637X/698/1/676. arXiv:0903.3416 [astro-ph.GA]

Dodds-Eden K, Sharma P, Quataert E et al (2010) Time-dependent models of flares from Sagittarius A*. ApJ 725(1):450–465. https://doi.org/10.1088/0004-637X/725/1/450. arXiv:1005.0389 [astro-ph.GA]

Dodds-Eden K, Gillessen S, Fritz TK et al (2011) The two states of Sgr A* in the near-infrared: bright episodic flares on top of low-level continuous variability. ApJ 728(1):37. https://doi.org/10.1088/0004-637X/728/1/37. arXiv:1008.1984 [astro-ph.GA]

Eckart A, Genzel R (1996) Observations of stellar proper motions near the Galactic Centre. Nature 383 (6599):415–417. https://doi.org/10.1038/383415a0

Eckart A, Baganoff FK, Schödel R et al (2006a) The flare activity of Sagittarius A*. New coordinated mm to X-ray observations. A&A 450(2):535–555. https://doi.org/10.1051/0004-6361:20054418. arXiv:astro-ph/0512440

Eckart A, Schödel R, Meyer L et al (2006b) Polarimetry of near-infrared flares from Sagittarius A*. A&A 455(1):1–10. https://doi.org/10.1051/0004-6361:20064948. arXiv:astro-ph/0610103

Einstein A (1916) Die Grundlage der allgemeinen Relativitätstheorie. Ann Phys 354(7):769–822. https://doi.org/10.1002/andp.19163540702

Eisenhauer F, Monnier JD, Pfuhl O (2023) Advances in optical/infrared interferometry. ARA&A 61:237–285. https://doi.org/10.1146/annurev-astro-121622-045019. arXiv:2303.00453 [astro-ph.IM]

Evans FA, Rasskazov A, Remmelzwaal A et al (2023) Constraints on the galactic centre environment from Gaia hypervelocity stars III: insights on a possible companion to Sgr A*. MNRAS 525(1):561–576. https://doi.org/10.1093/mnras/stad2273. arXiv:2304.12169 [astro-ph.GA]

Event Horizon Telescope Collaboration, Akiyama K, Algaba JC et al (2021a) First M87 Event Horizon Telescope results. VII. Polarization of the ring. ApJ 910(1):L12. https://doi.org/10.3847/2041-8213/abe71d. arXiv:2105.01169 [astro-ph.HE]

Event Horizon Telescope Collaboration, Akiyama K, Algaba JC et al (2021b) First M87 Event Horizon Telescope results. VIII. Magnetic field structure near the event horizon. ApJ 910(1):L13. https://doi.org/10.3847/2041-8213/abe4de. arXiv:2105.01173 [astro-ph.HE]

Event Horizon Telescope Collaboration, Akiyama K, Alberdi A et al (2022a) First Sagittarius A* Event Horizon Telescope results. I. The shadow of the supermassive black hole in the center of the Milky Way. ApJ 930(2):L12. https://doi.org/10.3847/2041-8213/ac6674

Event Horizon Telescope Collaboration, Akiyama K, Alberdi A et al (2022b) First Sagittarius A* Event Horizon Telescope results. V. Testing astrophysical models of the Galactic Center black hole. ApJ 930 (2):L16. https://doi.org/10.3847/2041-8213/ac6672

Fabian AC (2012) Observational evidence of active Galactic nuclei feedback. ARA&A 50:455–489. https://doi.org/10.1146/annurev-astro-081811-125521. arXiv:1204.4114 [astro-ph.CO]

Fabian AC, Iwasawa K (2000) Broad Fe-K lines from Seyfert galaxies. Adv Space Res 25(3–4):471–480. https://doi.org/10.1016/S0273-1177(99)00782-6

Falcke H, Markoff S (2000) The jet model for Sgr A*: radio and X-ray spectrum. A&A 362:113–118 arXiv:astro-ph/0102186

Falcke H, Melia F, Agol E (2000) Viewing the shadow of the black hole at the Galactic Center. ApJ 528(1): L13–L16. https://doi.org/10.1086/312423. arXiv:astro-ph/9912263

Ferrarese L, Merritt D (2000) A fundamental relation between supermassive black holes and their host galaxies. ApJ 539(1):L9–L12. https://doi.org/10.1086/312838. arXiv:astro-ph/0006053

Gebhardt K, Bender R, Bower G et al (2000) A relationship between nuclear black hole mass and galaxy velocity dispersion. ApJ 539(1):L13–L16. https://doi.org/10.1086/312840. arXiv:astro-ph/0006289

Genzel R, Townes CH (1987) Physical conditions, dynamics, and mass distribution in the center of the galaxy. ARA&A 25:377–423. https://doi.org/10.1146/annurev.aa.25.090187.002113

Genzel R, Hollenbach D, Townes CH (1994) The nucleus of our galaxy. Rep Prog Phys 57(5):417–479. https://doi.org/10.1088/0034-4885/57/5/001

Genzel R, Eckart A, Ott T et al (1997) On the nature of the dark mass in the centre of the Milky Way. MNRAS 291(1):219–234. https://doi.org/10.1093/mnras/291.1.219

Genzel R, Schödel R, Ott T et al (2003) Near-infrared flares from accreting gas around the supermassive black hole at the Galactic Centre. Nature 425(6961):934–937. https://doi.org/10.1038/nature02065. arXiv:astro-ph/0310821

Genzel R, Eisenhauer F, Gillessen S (2010) The Galactic Center massive black hole and nuclear star cluster. Rev Mod Phys 82(4):3121–3195. https://doi.org/10.1103/RevModPhys.82.3121. arXiv:1006.0064 [astro-ph.GA]

Ghez AM, Klein BL, Morris M et al (1998) High proper-motion stars in the vicinity of Sagittarius A*: evidence for a supermassive black hole at the center of our galaxy. ApJ 509(2):678–686. https://doi.org/10.1086/306528. arXiv:astro-ph/9807210

Ghez AM, Duchêne G, Matthews K et al (2003) The first measurement of spectral lines in a short-period star bound to the Galaxy's central black hole: a paradox of youth. ApJ 586(2):L127–L131. https://doi.org/10.1086/374804. arXiv:astro-ph/0302299

Ghez AM, Salim S, Weinberg NN et al (2008) Measuring distance and properties of the Milky Way's central supermassive black hole with stellar orbits. ApJ 689(2):1044–1062. https://doi.org/10.1086/592738. arXiv:0808.2870 [astro-ph]

Giacconi R (2003) Nobel lecture: the dawn of X-ray astronomy. Rev Mod Phys 75(3):995–1010. https://doi.org/10.1103/RevModPhys.75.995

Giacconi R, Gursky H, Paolini FR et al (1962) Evidence for X rays from sources outsideo the solar system. Phys. Rev. Lett. 9(11):439–443. https://doi.org/10.1103/PhysRevLett.9.439

Gillessen S, Eisenhauer F, Trippe S et al (2009) Monitoring stellar orbits around the massive black hole in the Galactic Center. ApJ 692(2):1075–1109. https://doi.org/10.1088/0004-637X/692/2/1075. arXiv:0810.4674 [astro-ph]

Gillessen S, Plewa PM, Eisenhauer F et al (2017) An update on monitoring stellar orbits in the Galactic Center. ApJ 837(1):30. https://doi.org/10.3847/1538-4357/aa5c41. arXiv:1611.09144 [astro-ph.GA]

Gillessen S, Plewa PM, Widmann F et al (2019) Detection of a drag force in G2's orbit: measuring the density of the accretion flow onto Sgr A* at 1000 Schwarzschild radii. ApJ 871(1):126. https://doi.org/10.3847/1538-4357/aaf4f8

Gondolo P, Silk J (1999) Dark matter annihilation at the Galactic Center. Phys Rev Lett 83(9):1719–1722. https://doi.org/10.1103/PhysRevLett.83.1719. arXiv:astro-ph/9906391

GRAVITY Collaboration, Abuter R, Accardo M et al (2017) First light for GRAVITY: phase referencing optical interferometry for the Very Large Telescope Interferometer. A&A 602:A94. https://doi.org/10.1051/0004-6361/201730838. arXiv:1705.02345 [astro-ph.IM]

GRAVITY Collaboration, Abuter R, Amorim A et al (2018a) Detection of the gravitational redshift in the orbit of the star S2 near the Galactic centre massive black hole. A&A 615:L15. https://doi.org/10.1051/0004-6361/201833718. arXiv:1807.09409 [astro-ph.GA]

GRAVITY Collaboration, Abuter R, Amorim A et al (2018b) Detection of orbital motions near the last stable circular orbit of the massive black hole SgrA*. A&A 618:L10. https://doi.org/10.1051/0004-6361/201834294. arXiv:1810.12641 [astro-ph.GA]

GRAVITY Collaboration, Sturm E, Dexter J et al (2018c) Spatially resolved rotation of the broad-line region of a quasar at sub-parsec scale. Nature 563(7733):657–660. https://doi.org/10.1038/s41586-018-0731-9. arXiv:1811.11195 [astro-ph.GA]

GRAVITY Collaboration, Abuter R, Amorim A et al (2019a) A geometric distance measurement to the Galactic center black hole with 0.3% uncertainty. A&A 625:L10. https://doi.org/10.1051/0004-6361/201935656. arXiv:1904.05721 [astro-ph.GA]

GRAVITY Collaboration, Amorim A, Bauböck M et al (2019b) Test of the Einstein equivalence principle near the Galactic Center supermassive black hole. Phys Rev Lett 122(10):101102. https://doi.org/10.1103/PhysRevLett.122.101102. arXiv:1902.04193 [astro-ph.GA]

GRAVITY Collaboration, Abuter R, Amorim A et al (2020a) The flux distribution of Sgr A*. A&A 638:A2. https://doi.org/10.1051/0004-6361/202037717. arXiv:2004.07185 [astro-ph.GA]

GRAVITY Collaboration, Abuter R, Amorim A et al (2020b) Detection of the schwarzschild precession in the orbit of the star S2 near the Galactic centre massive black hole. A&A 636:L5. https://doi.org/10.1051/0004-6361/202037813. arXiv:2004.07187 [astro-ph.GA]

GRAVITY Collaboration, Bauböck M, Dexter J et al (2020c) Modeling the orbital motion of Sgr A*'s near-infrared flares. A&A 635:A143. https://doi.org/10.1051/0004-6361/201937233. arXiv:2002.08374 [astro-ph.HE]

GRAVITY Collaboration, Jiménez-Rosales A, Dexter J et al (2020d) Dynamically important magnetic fields near the event horizon of Sgr A*. A&A 643:A56. https://doi.org/10.1051/0004-6361/202038283. arXiv:2009.01859 [astro-ph.HE]

GRAVITY Collaboration, Abuter R, Amorim A et al (2021) Constraining particle acceleration in Sgr A* with simultaneous GRAVITY, Spitzer, NuSTAR, and Chandra observations. A&A 654:A22. https://doi.org/10.1051/0004-6361/202140981. arXiv:2107.01096 [astro-ph.HE]

GRAVITY Collaboration, Abuter R, Aimar N et al (2022a) Deep images of the Galactic center with GRAVITY. A&A 657:A82. https://doi.org/10.1051/0004-6361/202142459. arXiv:2112.07477 [astro-ph.GA]

GRAVITY Collaboration, Abuter R, Aimar N et al (2022b) Mass distribution in the Galactic Center based on interferometric astrometry of multiple stellar orbits. A&A 657:L12. https://doi.org/10.1051/0004-6361/202142465. arXiv:2112.07478 [astro-ph.GA]

GRAVITY Collaboration, Abuter R, Aimar N et al (2023a) Polarimetry and astrometry of NIR flares as event horizon scale, dynamical probes for the mass of Sgr A*. A&A 677:L10. https://doi.org/10.1051/0004-6361/202347416. arXiv:2307.11821 [astro-ph.GA]

GRAVITY Collaboration, Straub O, Bauböck M et al (2023b) Where intermediate-mass black holes could hide in the Galactic Centre. A full parameter study with the S2 orbit. A&A 672:A63. https://doi.org/10.1051/0004-6361/202245132. arXiv:2303.04067 [astro-ph.GA]

GRAVITY Collaboration, Widmann F, Haubois X, et al (2024) Polarization analysis of the VLTI and GRAVITY. A&A 681:A115. https://doi.org/10.1051/0004-6361/202347238. arXiv:2311.03472 [astro-ph.IM]

GRAVITY+ Collaboration, Abuter R, Allouche F, et al (2022) First light for GRAVITY Wide. Large separation fringe tracking for the Very Large Telescope Interferometer. A&A 665:A75. https://doi.org/10.1051/0004-6361/202243941. arXiv:2206.00684 [astro-ph.IM]

GRAVITY+ Collaboration, Abuter R, Allouche F, et al (2024) A dynamical measure of the black hole mass in a quasar 11 billion years ago. Nature. https://doi.org/10.1038/s41586-024-07053-4. arXiv:2401.14567 [astro-ph.GA]

Greene JE, Seth A, den Brok M et al (2013) Using megamaser disks to probe black hole accretion. ApJ 771 (2):121. https://doi.org/10.1088/0004-637X/771/2/121. arXiv:1304.4254 [astro-ph.CO]

Greene JE, Seth A, Kim M et al (2016) Megamaser disks reveal a broad distribution of black hole mass in spiral galaxies. ApJ 826(2):L32. https://doi.org/10.3847/2041-8205/826/2/L32. arXiv:1606.00018 [astro-ph.GA]

Greene JE, Strader J, Ho LC (2020) Intermediate-mass black holes. ARA&A 58:257–312. https://doi.org/10.1146/annurev-astro-032620-021835. arXiv:1911.09678 [astro-ph.GA]

Gültekin K, Cackett EM, Miller JM et al (2009) The fundamental plane of accretion onto black holes with dynamical masses. ApJ 706(1):404–416. https://doi.org/10.1088/0004-637X/706/1/404. arXiv:0906.3285 [astro-ph.HE]

Haller JW, Rieke MJ, Rieke GH et al (1996) Stellar kinematics and the black hole in the Galactic Center. ApJ 456:194. https://doi.org/10.1086/176640

Häring N, Rix HW (2004) On the black hole mass-bulge mass relation. ApJ 604(2):L89–L92. https://doi.org/10.1086/383567. arXiv:astro-ph/0402376

Hasinger G (2020) Illuminating the dark ages: cosmic backgrounds from accretion onto primordial black hole dark matter. J Cosmol Astropart Phys 2020(7):022. https://doi.org/10.1088/1475-7516/2020/07/022. arXiv:2003.05150 [astro-ph.CO]

Hawking SW (1974) Black hole explosions? Nature 248(5443):30–31. https://doi.org/10.1038/248030a0

Hees A, Do T, Ghez AM et al (2017) Testing general relativity with stellar orbits around the supermassive black hole in our Galactic Center. Phys Rev Lett 118(21):211101. https://doi.org/10.1103/PhysRevLett.118.211101. arXiv:1705.07902 [astro-ph.GA]

Hees A, Do T, Roberts BM et al (2020) Search for a variation of the fine structure constant around the supermassive black hole in our Galactic Center. Phys Rev Lett 124(8):081101. https://doi.org/10.1103/PhysRevLett.124.081101. arXiv:2002.11567 [astro-ph.GA]

Ho PTP (1995) Molecular gas surrounding the galactic center. In: Winnewisser G, Pelz GC (eds) The physics and chemistry of interstellar molecular clouds. Lecture Notes in Physics, vol 459. Springer, Berlin, pp 33–40. https://doi.org/10.1007/BFb01020

Ho PTP, Ho LC, Szczepanski JC et al (1991) A molecular gas streamer feeding the Galactic Centre. Nature 350(6316):309–312. https://doi.org/10.1038/350309a0

Israel W (1967) Event horizons in static vacuum space-times. Phys Rev 164:1776–1779. https://doi.org/10.1103/PhysRev.164.1776

Issaoun S, Johnson MD, Blackburn L et al (2019) The size, shape, and scattering of Sagittarius A* at 86 GHz: first VLBI with ALMA. ApJ 871(1):30. https://doi.org/10.3847/1538-4357/aaf732. arXiv:1901.06226 [astro-ph.HE]

Johannsen T (2013) Photon rings around Kerr and Kerr-like black holes. ApJ 777(2):170. https://doi.org/10.1088/0004-637X/777/2/170. arXiv:1501.02814 [astro-ph.HE]

Johannsen T (2016) Sgr A* and general relativity. Class Quantum Gravity 33(11):113001. https://doi.org/10.1088/0264-9381/33/11/113001. arXiv:1512.03818 [astro-ph.GA]

Johannsen T, Wang C, Broderick AE et al (2016) Testing general relativity with accretion-flow imaging of Sgr A*. Phys Rev Lett 117(9):091101. https://doi.org/10.1103/PhysRevLett.117.091101. arXiv:1608.03593 [astro-ph.HE]

Johnson MD, Lupsasca A, Strominger A et al (2020) Universal interferometric signatures of a black hole's photon ring. Sci Adv 6(12):eaaz1310. https://doi.org/10.1126/sciadv.aaz1310. arXiv:1907.04329 [astro-ph.IM]

Jovanović P, et al (2024) Improvement of graviton mass constraints using GRAVITY's detection of Schwarzschild precession in the orbit of S2 star around the Galactic Center. Phys Rev D. arXiv:2305.13448 [astro-ph.GA]

Kaspi S, Smith PS, Netzer H et al (2000) Reverberation measurements for 17 quasars and the size-mass-luminosity relations in active galactic nuclei. ApJ 533(2):631–649. https://doi.org/10.1086/308704. arXiv:astro-ph/9911476

Kerr RP (1963) Gravitational field of a spinning mass as an example of algebraically special metrics. Phys Rev Lett 11:237–238. https://doi.org/10.1103/PhysRevLett.11.237

Kormendy J (2004) The stellar-dynamical search for supermassive black holes in galactic nuclei. In: Ho LC (ed) Coevolution of black holes and galaxies. Cambridge University Press, pp 1–20 arXiv:astro-ph/0306353

Kormendy J, Ho LC (2013) Coevolution (or not) of supermassive black holes and host galaxies. ARA&A 51(1):511–653. https://doi.org/10.1146/annurev-astro-082708-101811. arXiv:1304.7762 [astro-ph.CO]

Kormendy J, Kennicutt RC Jr (2004) Secular evolution and the formation of pseudobulges in disk galaxies. ARA&A 42(1):603–683. https://doi.org/10.1146/annurev.astro.42.053102.134024. arXiv:0407343 [astro-ph]

Krabbe A, Genzel R, Eckart A et al (1995) The nuclear cluster of the Milky Way: star formation and velocity dispersion in the central 0.5 parsec. ApJ 447:L95. https://doi.org/10.1086/309579

Lacroix T (2018) Dynamical constraints on a dark matter spike at the Galactic centre from stellar orbits. A&A 619:A46. https://doi.org/10.1051/0004-6361/201832652. arXiv:1801.01308 [astro-ph.GA]

Lacy JH, Townes CH, Geballe TR et al (1980) Observations of the motion and distribution of the ionized gas in the central parsec of the Galaxy. II. ApJ 241:132–146. https://doi.org/10.1086/158324

Laplace PS (1795) Exposition du système du monde, vol 2. Imprimerie du Cercle Social, Paris. https://gallica.bnf.fr/ark:/12148/bpt6k1050382f

Linial I, Sari R (2022) Stellar distributions around a supermassive black hole: strong-segregation regime revisited. ApJ 940(2):101. https://doi.org/10.3847/1538-4357/ac9bfd. arXiv:2206.14817 [astro-ph.GA]

Lo KY, Claussen MJ (1983) High-resolution observations of ionized gas in central 3 parsecs of the Galaxy: possible evidence for infall. Nature 306(5944):647–651. https://doi.org/10.1038/306647a0

Lu W, Kumar P, Narayan R (2017) Stellar disruption events support the existence of the black hole event horizon. MNRAS 468(1):910–919. https://doi.org/10.1093/mnras/stx542. arXiv:1703.00023 [astro-ph.HE]

Luminet JP (1979) Image of a spherical black hole with thin accretion disk. A&A 75:228–235

Lynden-Bell D (1969) Galactic nuclei as collapsed old quasars. Nature 223(5207):690–694. https://doi.org/10.1038/223690a0

Lynden-Bell D, Rees MJ (1971) On quasars, dust and the galactic centre. MNRAS 152:461. https://doi.org/10.1093/mnras/152.4.461

Magorrian J, Tremaine S, Richstone D et al (1998) The demography of massive dark objects in Galaxy Centers. AJ 115(6):2285–2305. https://doi.org/10.1086/300353. arXiv:astro-ph/9708072

Maiolino R, Scholtz J, Witstok J, et al (2024) A small and vigorous black hole in the early Universe. Nature 627:59–63. https://doi.org/10.1038/s41586-024-07052-5. arXiv:2305.12492 [astro-ph.GA]

Maldacena J (1998) The large N limit of superconformal field theories and supergravity. Adv Theor Math Phys 2:231. https://doi.org/10.4310/ATMP.1998.v2.n2.a1

Maoz E (1995) A stringent constraint on alternatives to a massive black hole at the center of NGC 4258. ApJ 447:L91. https://doi.org/10.1086/309574. arXiv:astro-ph/9503113
Marrone DP, Moran JM, Zhao JH et al (2007) An unambiguous detection of faraday rotation in Sagittarius A*. ApJ 654(1):L57–L60. https://doi.org/10.1086/510850. arXiv:astro-ph/0611791
Matsumoto T, Chan CH, Piran T (2020) The origin of hotspots around Sgr A*: orbital or pattern motion? MNRAS 497(2):2385–2392. https://doi.org/10.1093/mnras/staa2095. arXiv:2004.13029 [astro-ph.HE]
Mazur PO, Mottola E (2004) Gravitational vacuum condensate stars. Proc Natl Acad Sci 101(26):9545–9550. https://doi.org/10.1073/pnas.0402717101. arXiv:gr-qc/0407075
McClintock JE, Remillard RA (2006) Black hole binaries. In: Lewin W, van der Klis M (eds) Compact stellar X-ray sources. Cambridge University Press, Cambridge, pp 157–214. https://doi.org/10.1017/CBO9780511536281.005
McConnell NJ, Ma CP (2013) Revisiting the scaling relations of black hole masses and host galaxy properties. ApJ 764(2):184. https://doi.org/10.1088/0004-637X/764/2/184. arXiv:1211.2816 [astro-ph.CO]
McGinn MT, Sellgren K, Becklin EE et al (1989) Stellar kinematics in the Galactic Center. ApJ 338:824. https://doi.org/10.1086/167239
Melia F, Falcke H (2001) The supermassive black hole at the galactic center. ARA&A 39:309–352. https://doi.org/10.1146/annurev.astro.39.1.309. arXiv:astro-ph/0106162
Merritt D (2010) The distribution of Stars and Stellar remnants at the Galactic Center. ApJ 718(2):739–761. https://doi.org/10.1088/0004-637X/718/2/739. arXiv:0909.1318 [astro-ph.GA]
Merritt D, Alexander T, Mikkola S et al (2010) Testing properties of the Galactic center black hole using stellar orbits. Phys. Rev. D 81(6):062002. https://doi.org/10.1103/PhysRevD.81.062002. arXiv:0911.4718 [astro-ph.GA]
Michell J (1784) On the means of discovering the distance, magnitude, &c. of the fixed stars, in consequence of the diminution of the velocity of their light, in case such a diminution should be found to take place in any of them, and such other data should be procured from observations, as would be farther necessary for that purpose. Philos Trans R Soc Lond Ser I 74:35–57. https://doi.org/10.1098/rstl.1784.0008
Michelson A, Morley E (1887) On the relative motion of the earth and the luminiferous ether. Am J Sci 34 (203):333–345. https://doi.org/10.2475/ajs.s3-34.203.333
Miyoshi M, Moran J, Herrnstein J et al (1995) Evidence for a black hole from high rotation velocities in a sub-parsec region of NGC4258. Nature 373(6510):127–129. https://doi.org/10.1038/373127a0
Moran JM (2008) The black-hole accretion disk in NGC 4258: one of nature's most beautiful dynamical systems. In: Bridle AH, Condon JJ, Hunt GC (eds) Frontiers of astrophysics: a celebration of NRAO's 50th Anniversary, ASP Conference Series, vol 395. Astronomical Society of the Pacific, pp 87. arXiv:0804.1063
Morris M, Serabyn E (1996) The Galactic Center environment. ARA&A 34:645–702. https://doi.org/10.1146/annurev.astro.34.1.645
Morris MS, Thorne KS (1988) Wormholes in spacetime and their use for interstellar travel. Am J Phys 56:395. https://doi.org/10.1119/1.15620
Morris MR, Meyer L, Ghez AM (2012) Galactic center research: manifestations of the central black hole. Res Astron Astrophys 12(8):995–1020. https://doi.org/10.1088/1674-4527/12/8/007. arXiv:1207.6755 [astro-ph.GA]
Munyaneza F, Tsiklauri D, Viollier RD (1999) Dynamics of the Star S0–1 and the nature of the compact dark object at the Galactic Center. ApJ 526(2):744–751. https://doi.org/10.1086/308026. arXiv:astro-ph/9903242
Nandra K, George IM, Mushotzky RF et al (1997) ASCA observations of Seyfert 1 galaxies. II. Relativistic iron Kα emission. ApJ 477(2):602–622. https://doi.org/10.1086/303721. arXiv:astro-ph/9606169
Netzer H (2013) The physics and evolution of active galactic nuclei. Cambridge University Press, Cambridge. https://doi.org/10.1017/CBO9781139109291
Netzer H (2015) Revisiting the unified model of active galactic nuclei. ARA&A 53:365–408. https://doi.org/10.1146/annurev-astro-082214-122302. arXiv:1505.00811 [astro-ph.GA]
Netzer H (2020) Testing broad-line region models with reverberation mapping. MNRAS 494(2):1611–1621. https://doi.org/10.1093/mnras/staa767. arXiv:2003.07660 [astro-ph.GA]
Newman ET et al (1965) Metric of a rotating, charged mass. J Math Phys 6:918. https://doi.org/10.1063/1.1704351

Olivares H, Younsi Z, Fromm CM et al (2020) How to tell an accreting boson star from a black hole. MNRAS 497(1):521–535. https://doi.org/10.1093/mnras/staa1878. arXiv:1809.08682 [gr-qc]
Oort JH (1977) The galactic center. ARA&A 15:295–362. https://doi.org/10.1146/annurev.aa.15.090177.001455
Oppenheimer JR, Snyder H (1939) On continued gravitational contraction. Phys Rev 56(5):455–459. https://doi.org/10.1103/PhysRev.56.455
Osmer PS (2004) The evolution of quasars. In: Ho LC (ed) Coevolution of BHs and galaxies, carnegie observatories astrophysics series, vol 1. Cambridge University Press, Cambridge, pp 324–340
Özel F, Psaltis D, Narayan R et al (2010) The black hole mass distribution in the galaxy. ApJ 725(2):1918–1927. https://doi.org/10.1088/0004-637X/725/2/1918. arXiv:1006.2834 [astro-ph.GA]
Penrose R (1963) Asymptotic properties of fields and space-times. Phys Rev Lett 10:66–68. https://doi.org/10.1103/PhysRevLett.10.66
Penrose R (1965) Gravitational collapse and space-time singularities. Phys Rev Lett 14:57–59. https://doi.org/10.1103/PhysRevLett.14.57
Peterson BM (2014) Measuring the masses of supermassive black holes. Space Sci Rev 183(1–4):253–275. https://doi.org/10.1007/s11214-013-9987-4
Ponti G, George E, Scaringi S et al (2017) A powerful flare from Sgr A* confirms the synchrotron nature of the X-ray emission. MNRAS 468(2):2447–2468. https://doi.org/10.1093/mnras/stx596. arXiv:1703.03410 [astro-ph.HE]
Portegies Zwart SF, Boekholt TCN, Heggie DC (2023) Punctuated chaos and the unpredictability of the Galactic Centre S-star orbital evolution. MNRAS 526(4):5791–5799. https://doi.org/10.1093/mnras/stad2654. arXiv:2308.14817 [astro-ph.GA]
Psaltis D (2024) Black holes in classical general relativity and beyond. In: Haiman Z (ed) The encyclopedia of cosmology, set 2: frontiers in cosmology. Volume 3: black holes. World Scientific, Singapore, pp 1–25. https://doi.org/10.1142/9789811282676_0001arXiv:2304.09984
Psaltis D, Johannsen T (2011) Sgr A*: the optimal testbed of strong-field gravity. J Phys Conf Ser 283:012030. https://doi.org/10.1088/1742-6596/283/1/012030. arXiv:1012.1602 [astro-ph.HE]
Psaltis D, Wex N, Kramer M (2016) A quantitative test of the no-hair theorem with Sgr A* using stars, pulsars, and the event horizon telescope. ApJ 818(2):121. https://doi.org/10.3847/0004-637X/818/2/121. arXiv:1510.00394 [astro-ph.HE]
Quataert E (2004) A dynamical model for hot gas in the Galactic Center. ApJ 613(1):322–325. https://doi.org/10.1086/422973. arXiv:0310446 [astro-ph]
Quataert E, Gruzinov A (2000) Constraining the accretion rate onto Sagittarius A* using linear polarization. ApJ 545(2):842–846. https://doi.org/10.1086/317845. arXiv:0004286 [astro-ph]
Rees MJ (1984) Black hole models for active galactic nuclei. ARA&A 22:471–506. https://doi.org/10.1146/annurev.aa.22.090184.002351
Remillard RA, McClintock JE (2006) X-ray properties of black-hole binaries. ARA&A 44(1):49–92. https://doi.org/10.1146/annurev.astro.44.051905.092532. arXiv:0606352 [astro-ph]
Ressler SM, Quataert E, Stone JM (2018) Hydrodynamic simulations of the inner accretion flow of Sagittarius A* fuelled by stellar winds. MNRAS 478(3):3544–3563. https://doi.org/10.1093/mnras/sty1146. arXiv:1805.00474 [astro-ph.HE]
Ressler SM, Quataert E, Stone JM (2020a) The surprisingly small impact of magnetic fields on the inner accretion flow of Sagittarius A* fueled by stellar winds. MNRAS 492(3):3272–3293. https://doi.org/10.1093/mnras/stz3605. arXiv:2001.04469 [astro-ph.HE]
Ressler SM, White CJ, Quataert E et al (2020b) Ab initio horizon-scale simulations of magnetically arrested accretion in Sagittarius A* fed by stellar winds. ApJ 896(1):L6. https://doi.org/10.3847/2041-8213/ab9532. arXiv:2006.00005 [astro-ph.HE]
Reynolds CS (2021) Observational constraints on black hole spin. ARA&A 59:117–154. https://doi.org/10.1146/annurev-astro-112420-035022. arXiv:2011.08948 [astro-ph.HE]
Rezzolla L, Most ER, Weih LR (2018) Using gravitational-wave observations and quasi-universal relations to constrain the maximum mass of neutron stars. ApJ 852(2):L25. https://doi.org/10.3847/2041-8213/aaa401. arXiv:1711.00314 [astro-ph.HE]
Robinson DC (1975) Uniqueness of the Kerr Black Hole. Phys Rev Lett 34(14):905–906. https://doi.org/10.1103/PhysRevLett.34.905
Rosa JaL, Garcia P, Vincent FH et al (2022) Observational signatures of hot spots orbiting horizonless objects. Phys Rev D 106:044031. https://doi.org/10.1103/PhysRevD.106.044031
Ruffini R, Argüelles CR, Rueda JA (2015) On the core-halo distribution of dark matter in galaxies. MNRAS 451(1):622–628. https://doi.org/10.1093/mnras/stv1016. arXiv:1409.7365 [astro-ph.GA]

Sadeghian L, Ferrer F, Will CM (2013) Dark-matter distributions around massive black holes: a general relativistic analysis. Phys Rev D 88(6):063522. https://doi.org/10.1103/PhysRevD.88.063522. arXiv:1305.2619 [astro-ph.GA]

Saglia RP, Opitsch M, Erwin P et al (2016) The SINFONI black hole survey: the black hole fundamental plane revisited and the paths of (co)evolution of supermassive black holes and bulges. ApJ 818(1):47. https://doi.org/10.3847/0004-637X/818/1/47. arXiv:1601.00974 [astro-ph.GA]

Schmidt M (1963) 3C 273: a star-like object with large red-shift. Nature 197(4872):1040. https://doi.org/10.1038/1971040a0

Schneider R, Valiante R, Trinca A et al (2023) Are we surprised to find SMBHs with JWST at z $\geq$ 9? MNRAS 526(3):3250–3261. https://doi.org/10.1093/mnras/stad2503. arXiv:2305.12504 [astro-ph.GA]

Schödel R, Ott T, Genzel R et al (2002) A star in a 15.2-year orbit around the supermassive black hole at the centre of the Milky Way. Nature 419(6908):694–696. https://doi.org/10.1038/nature01121. arXiv:0210426 [astro-ph]

Schwarzschild K (1916) On the gravitational field of a mass point according to Einstein's theory. Sitzungsber Preuss Akad Wiss Phys Math Kl 1916:189–196. https://doi.org/10.1023/A:1022971926521 (Transl. reprinted in Gen Relativ Gravit 35:951 (2003))

Serabyn E, Lacy JH (1985) NE II observations of the galactic center: evidence for a massive black hole. ApJ 293:445–458. https://doi.org/10.1086/163250

Shakura NI, Sunyaev RA (1973) Black holes in binary systems. Observational appearance. A&A 24:337–355

Susskind L (1995) The world as a hologram. J Math Phys 36(11):6377–6396. https://doi.org/10.1063/1.531249. arXiv:hep-th/9409089

Tanaka Y, Nandra K, Fabian AC et al (1995) Gravitationally redshifted emission implying an accretion disk and massive black hole in the active galaxy MCG-6-30-15. Nature 375(6533):659–661. https://doi.org/10.1038/375659a0

Thompson RA, Moran JM, Swenson GW Jr (2017) Interferometry and synthesis in radio astronomy, 3rd edn. Springer, Cham. https://doi.org/10.1007/978-3-319-44431-4

Torres DF, Capozziello S, Lambiase G (2000) Supermassive boson star at the galactic center? Phys Rev D 62(10):104012. https://doi.org/10.1103/PhysRevD.62.104012. arXiv:astro-ph/0004064

Tsiklauri D, Viollier RD (1998) Dark matter concentration in the Galactic Center. ApJ 500(2):591–595. https://doi.org/10.1086/305753. arXiv:astro-ph/9805273

Vestergaard M, Osmer PS (2009) Mass functions of the active black holes in distant quasars from the large bright quasar survey, the bright quasar survey, and the color-selected sample of the SDSS fall equatorial stripe. ApJ 699(1):800–816. https://doi.org/10.1088/0004-637X/699/1/800. arXiv:0904.3348 [astro-ph.CO]

Vestergaard M, Fan X, Tremonti CA et al (2008) Mass functions of the active black holes in distant quasars from the Sloan Digital Sky Survey Data Release 3. ApJ 674(1):L1. https://doi.org/10.1086/528981. arXiv:0801.0243 [astro-ph]

Vincent FH, Meliani Z, Grandclément P et al (2016) Imaging a boson star at the Galactic center. Class Quantum Gravity 33(10):105015. https://doi.org/10.1088/0264-9381/33/10/105015. arXiv:1510.04170 [gr-qc]

Viollier RD, Trautmann D, Tupper GB (1993) Supermassive neutrino stars and galactic nuclei. Phys Lett B 306(1–2):79–85. https://doi.org/10.1016/0370-2693(93)91141-9

Waisberg I, Dexter J, Gillessen S et al (2018) What stellar orbit is needed to measure the spin of the Galactic centre black hole from astrometric data? MNRAS 476(3):3600–3610. https://doi.org/10.1093/mnras/sty476. arXiv:1802.08198 [astro-ph.GA]

Wheeler JA (1968) Our universe: the known and the unknown. Am Sci 56(1):1–20

Wielgus M, Moscibrodzka M, Vos J et al (2022) Orbital motion near Sagittarius A*. Constraints from polarimetric ALMA observations. A&A 665:L6. https://doi.org/10.1051/0004-6361/202244493. arXiv:2209.09926 [astro-ph.HE]

Will CM (2008) Testing the general relativistic no-hair theorems using the galactic center black hole Sagittarius A*. ApJ 674(1):L25. https://doi.org/10.1086/528847. arXiv:0711.1677 [astro-ph]

Will CM, Naoz S, Hees A et al (2023) Constraining a companion of the galactic center black hole Sgr A*. ApJ 959(1):58. https://doi.org/10.3847/1538-4357/ad09b3. arXiv:2307.16646 [astro-ph.GA]

Witzel G, Eckart A, Bremer M et al (2012) Source-intrinsic near-infrared properties of Sgr A*: total intensity measurements. ApJS 203(2):18. https://doi.org/10.1088/0067-0049/203/2/18. arXiv:1208.5836 [astro-ph.HE]

Witzel G, Martinez G, Hora J et al (2018) Variability timescale and spectral index of Sgr A* in the near infrared: approximate bayesian computation analysis of the variability of the closest supermassive black hole. ApJ 863(1):15. https://doi.org/10.3847/1538-4357/aace62. arXiv:1806.00479 [astro-ph.HE]

Witzel G, Martinez G, Willner SP et al (2021) Rapid variability of Sgr A* across the electromagnetic spectrum. ApJ 917(2):73. https://doi.org/10.3847/1538-4357/ac0891. arXiv:2011.09582 [astro-ph.HE]

Wollman ER, Geballe TR, Lacy JH et al (1977) Ne II 12.8 micron emission from the galactic center. II. ApJ 218:L103–L107. https://doi.org/10.1086/182585

Yuan F, Narayan R (2014) Hot accretion flows around black holes. ARA&A 52:529–588. https://doi.org/10.1146/annurev-astro-082812-141003. arXiv:1401.0586 [astro-ph.HE]

Yuan F, Quataert E, Narayan R (2003) Nonthermal electrons in radiatively inefficient accretion flow models of Sagittarius A*. ApJ 598(1):301–312. https://doi.org/10.1086/378716. arXiv:astro-ph/0304125

Zakharov AF, Nucita AA, de Paolis F et al (2007) Apoastron shift constraints on dark matter distribution at the Galactic Center. Phys. Rev. D 76(6):062001. https://doi.org/10.1103/PhysRevD.76.062001. arXiv:0707.4423 [astro-ph]

Zhang YP, Zeng YB, Wang YQ et al (2022) Motion of test particle in rotating boson star. Phys Rev D 105:044021. https://doi.org/10.1103/PhysRevD.105.044021

Authors and Affiliations

Reinhard Genzel[1,2,3] · Frank Eisenhauer[1,4] · Stefan Gillessen[1]

✉ Reinhard Genzel
genzel@mpe.mpg.de

Frank Eisenhauer
eisenhau@mpe.mpg.de

Stefan Gillessen
ste@mpe.mpg.de

[1] Max-Planck Institute for Extraterrestrial Physics, Gießenbachstr. 1, 85748 Garching, Germany

[2] Departments of Physics and Astronomy, University of California, Le Conte Hall, Berkeley, CA 94720, USA

[3] Faculty of Physics, Ludwig Maximilian University, Munich, Germany

[4] Department of Physics, TUM School of Natural Sciences, Technical University of Munich, 85748 Garching, Germany